

**Norwegian University of Life Sciences**

Faculty of Environmental Sciences and Natural Resource Management

**2023**

ISSN 2535-2806

MINA fagrapport 89

# **Estimates of wolverine density, abundance, and population dynamics in Scandinavia, 2014–2023**

Cyril Milleret  
Pierre Dupont  
Henrik Brøseth  
Øystein Flagstad  
Oddmund Kleven  
Jonas Kindberg  
Richard Bischof



Milleret, C., Dupont, P., Brøseth, H., Flagstad, Ø, Kleven, O., Kindberg, J., and Bischof, R., 2023. **Estimates of wolverine density, abundance, and population dynamics in Scandinavia, 2014–2023** - MINA fagrapport 89. 33 pp.

Ås, December 2023

ISSN: 2535-2806

COPYRIGHT

© Norwegian University of Life Sciences (NMBU)

The publication may be freely cited where the source is acknowledged

AVAILABILITY

Open

PUBLICATION TYPE

Digital document (pdf)

QUALITY CONTROLLED BY

The Research committee (FU), MINA, NMBU

PRINCIPAL

Naturvårdsverket, Ref: NV-366-23-005, Contact person: Robert Ekblom

Miljødirektoratet, Ref: 22047026, Contact person: Terje Bø

COVER PICTURE

Wolverine, Ridgeline plot of wolverine density in Norway and Sweden

NØKKELOORD

*Gulo gulo*, jerv, tetthet, populasjonsdynamikk, deteksjonssannsynlighet, ikke-invaserende innsamling av genetisk materiale, åpen populasjon romlig fangst-gjenfangst, rovdyrforvaltning

KEY WORDS

*Gulo gulo*, wolverine, population density, population dynamics, detection probability, non-invasive genetic sampling, open-population spatial capture-recapture, carnivore management

Cyril Milleret, Faculty of Environmental Sciences and Natural Resource Management, Norwegian University of Life Sciences, PO Box 5003, NO-1432 Ås, Norway

Pierre Dupont, Faculty of Environmental Sciences and Natural Resource Management, Norwegian University of Life Sciences, PO Box 5003, NO-1432 Ås, Norway

Henrik Brøseth, Norwegian Institute for Nature Research, PO Box 5685, NO-7485 Trondheim, Norway

Øystein Flagstad, Norwegian Institute for Nature Research, PO Box 5685, NO-7485 Trondheim, Norway

Oddmund Kleven, Norwegian Institute for Nature Research, PO Box 5685, NO-7485 Trondheim, Norway

Jonas Kindberg, Norwegian Institute for Nature Research, PO Box 5685, NO-7485 Trondheim, Norway

Richard Bischof ([richard.bischof@nmbu.no](mailto:richard.bischof@nmbu.no)), Faculty of Environmental Sciences and Natural Resource Management, Norwegian University of Life Sciences, PO Box 5003, NO-1432 Ås, Norway

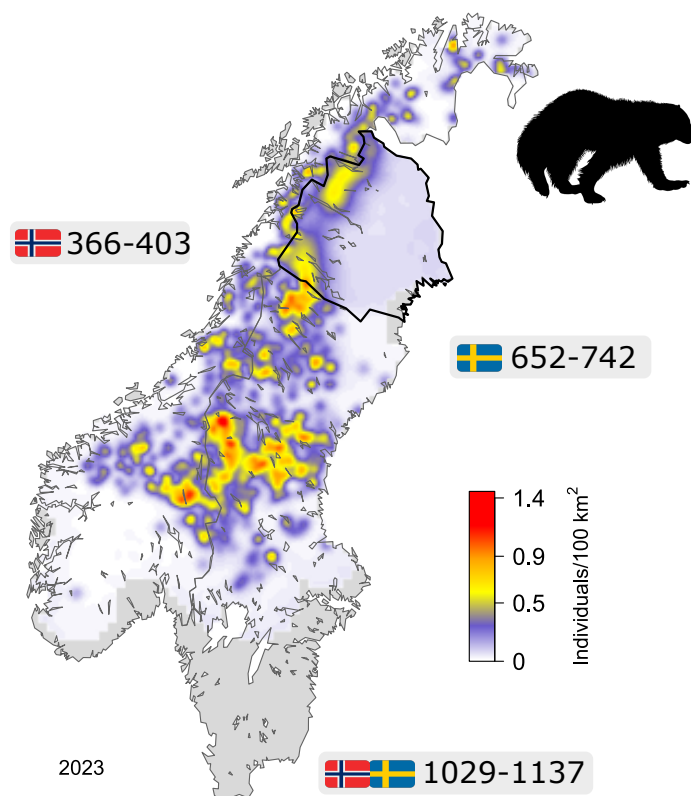
## Summary

**Background** The Scandinavian wolverine (*Gulo gulo*) population is being monitored annually using non-invasive genetic sampling (NGS) and recovery of dead individuals. DNA extracted from feces, urine, hair, secretion, and tissue is used to identify the species, sex, and individual from which each sample originated. These data have been compiled in the Scandinavian large carnivore database Rovbase 3.0. ([www.rovbase.se](http://www.rovbase.se), [www.rovbase.no](http://www.rovbase.no)).

**Approach** Using the Bayesian open-population spatial capture-recapture (OPSCR) model developed by RovQuant, we estimated annual density, total and jurisdiction-specific population sizes and vital rates of the Scandinavian wolverine population for ten consecutive seasons from 2014 to 2023.

**Results** We generated annual density maps and estimated total and jurisdiction-specific population sizes for the wolverine during 2014 to 2023. Based on the OPSCR model, the size of the Scandinavian wolverine population was likely (95% Bayesian credible interval) between 1029 and 1137 individuals in 2023, with 652 to 742 individuals attributed to Sweden and 366 to 403 to Norway. In addition to annual density and abundance estimates, we report, for each sex, annual estimates of cause-specific mortality, recruitment, and detection probability.

**Discussion** While overall abundance estimates remained relatively stable between 2022 and 2023, there was a significant drop in the estimated survival of female wolverines. According to the model, this apparent drop was attributable to an increase in mortality due to causes other than legal hunting, including natural deaths, collisions, and unreported human-caused deaths. Further research is needed to determine if this finding is the result of an analytical artifact, a change in monitoring that was unaccounted for in the model, or a true drop in female survival.



Density map and ranges of abundance estimated for wolverines in 2023

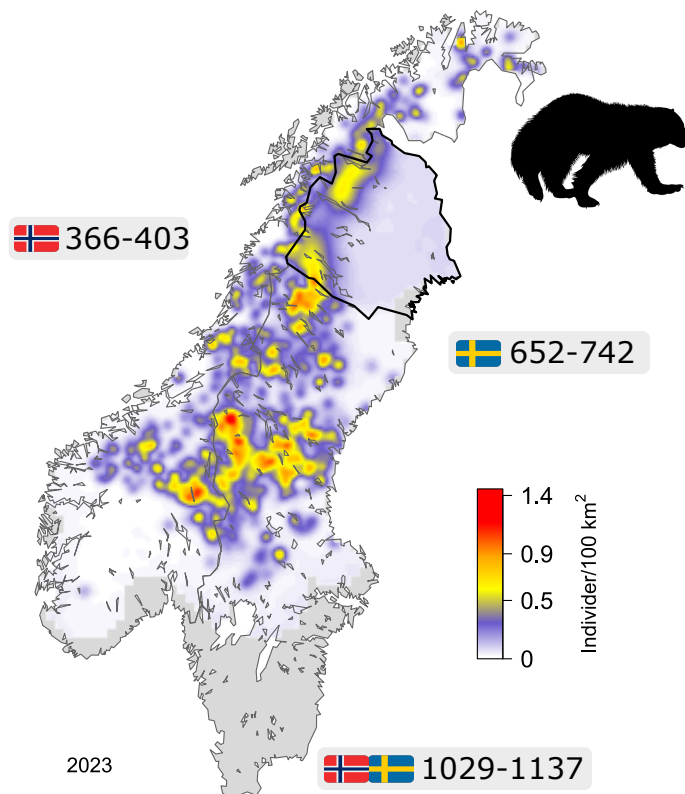
## Sammendrag

**Bakgrunn** Den skandinaviske bestanden av jerv (*Gulo gulo*) blir overvåket årlig ved bruk av ikke-invasiv genetisk prøveinnsamling (NGS) og gjenfunn av døde individer. DNA ekstrahert fra skit, urin, hår og vev brukes til å identifisere art, kjønn og individ for hver enkelt prøve. Denne informasjonen samles og ivaretas i den skandinaviske databasen for store rovdyr; Rovbase 3.0 ([www.rovbase.se](http://www.rovbase.se), [www.rovbase.no](http://www.rovbase.no)).

**Tilnærming** Ved bruk av en Bayesiansk åpen romlig fangst-gjenfangst populasjons modell (OPSCR), utviklet av RovQuant, estimerte vi årlige tettheter og demografiske rater hos den skandinaviske jervebestanden i ti sesonger fra 2014 til 2023.

**Resultater** Vi laget årlige kart med tetthet av jerv fra 2014 til 2023, hvor bestandsstørrelsen både totalt og innenfor ulike administrative enheter kunne avledes. Basert på OPSCR modellen var den skandinaviske bestanden av jerv mellom 1029 og 1137 individer i 2023 (95% kredibelt intervall), med 652 til 742 individer i Sverige og 366 til 403 individer i Norge. I tillegg til årlige tettheter og områdespesifikke bestandsestimater, gir rapporten estimater på dødlighetsfaktorer, rekruttering og oppdagbarhet.

**Diskusjon** Selv om bestandsestimatene er relativt stabile mellom 2022 og 2023 viser resultatene fra modellen en vesentlig reduksjon i overlevelsen til hunner. Den reduserte overlevelsen skyldes en økning i dødeligheten som følge av faktorer utenom lovlig jakt, slik som naturlig dødelighet, kollisjoner og urapportert menneskeskapt dødelighet. Videre analyser er påkrevd for å finne ut om dette er en artefakt av analysen, et resultat av endring i overvåkingen som ikke ble hensyntatt i modelleringen, eller en reell nedgang i overlevelse hos hunner



Kart som viser tetthet av jerv i 2023 sammen med intervaller for estimert antall jerv

# Contents

<b>1</b>	<b>Introduction</b>	<b>6</b>
<b>2</b>	<b>Methods</b>	<b>8</b>
2.1	Data . . . . .	8
2.2	Open-population spatial capture-recapture model . . . . .	9
<b>3</b>	<b>Results</b>	<b>13</b>
3.1	Non-invasive genetic samples and dead recoveries . . . . .	13
3.2	Density and abundance . . . . .	13
3.3	Vital rates . . . . .	15
3.4	Detection probability . . . . .	16
<b>4</b>	<b>Discussion</b>	<b>17</b>
<b>5</b>	<b>Summary and suggestions of improvements</b>	<b>19</b>
5.1	Summary of improvements made . . . . .	19
5.2	Suggestions for future improvements . . . . .	19
5.3	Other recommendations . . . . .	19
<b>6</b>	<b>Acknowledgements</b>	<b>20</b>
<b>7</b>	<b>Data availability</b>	<b>20</b>
	<b>References</b>	<b>22</b>
	<b>Appendices</b>	<b>23</b>

# 1 Introduction

Sweden and Norway monitor large carnivores using non-invasive genetic sampling (NGS) and dead recoveries. Both countries have collected an extensive individual-based data set for the wolverine (*Gulo gulo*), which is stored in the Scandinavian large carnivore database Rovbase ([www.rovbase.se](http://www.rovbase.se), [www.rovbase.no](http://www.rovbase.no)). Since 2017, project RovQuant has been developing statistical methods that allow a comprehensive assessment of the status and dynamics of large carnivore populations using NGS data and other sources of information stored in Rovbase (Bischof et al., 2019b, 2020b). The analytical framework developed by RovQuant is based on Bayesian open-population spatial capture-recapture (OPSCR) models (Ergon and Gardner, 2014; Bischof et al., 2016; Chandler et al., 2018). These models use the spatial and temporal information contained in the repeated genetic detections of individuals to estimate various population parameters, including spatially-explicit abundance (i.e., density) and vital rates (e.g., recruitment and survival). Importantly, the approach accounts for imperfect detection during sampling (i.e., the fact that some individuals are not detected at all) and animal movement (i.e., the fact that individuals may use and be detected in multiple management units or countries). The OPSCR method brings along several advantages, including the ability to map density, derive jurisdiction-specific abundance, estimate survival and recruitment (which are needed for making population projections), and yield tractable measures of uncertainty (Bischof et al., 2019a, 2020b).

RovQuant reported abundance estimates for wolverines and wolves (*Canis lupus*) on an annual basis since 2019 (Bischof et al., 2019a,b, 2020b; Milleret et al., 2021b, 2022b,d; Flagstad et al., 2021; Milleret et al., 2023, 2022c) and for brown bears (*Ursus arctos* in Norway since 2022 (Dupont et al., 2022, 2023)). During these and other analyses (Milleret et al., 2018, 2019; Bischof et al., 2020a; Dupont et al., 2021; Turek et al., 2021; Dey et al., 2022), RovQuant has continuously improved the performance of the OPSCR models. In the present report, we summarize the analysis of a 10-year time series (2014–2023) using the latest available wolverine monitoring data (Kleven et al., 2023) and the most recent version of the OPSCR model. We provide the following information:

- Annual and sex-specific estimates of the number of wolverines for Sweden, Norway, and both countries combined, as well as estimates by county in Sweden and by carnivore management region in both countries.
- Annual maps of wolverine density throughout the species' range in Scandinavia.
- Annual and sex-specific estimates of survival, cause-specific mortality, recruitment, and population growth rate.
- Estimated proportion of individuals detected through non-invasive genetic sampling.

All estimates are accompanied by their 95% Bayesian credible intervals.

## Box 1: Terms and acronyms used

**AC:** Activity center. Model-based equivalent of the center of an individual's home range during the monitoring period. "AC location" refers to the spatial coordinates of an individual AC in a given year and "AC movement" to the movement of an individual AC between consecutive years.

**CrI:** 95% credible interval associated with a posterior sample distribution.

**Detectors:** Potential detection locations in the spatial capture-recapture framework. These can refer to fixed locations (e.g., camera-trap locations) or in this report to areas searched (e.g., habitat grid cells where searches for genetic samples were conducted). The searched area was defined as a 90 km buffer around all NGS data collected during the period considered.

**Statsforvalteren:** Norwegian state's representative in the county, responsible for following up decisions, goals, and guidelines from the legislature and the government.

**Habitat buffer:** Buffer surrounding the searched area that is considered potentially suitable habitat but was not searched (60km in this report).

**Legal culling:** Lethal removal of individuals by legal means, including licensed recreational hunting, management removals, and defense of life and property.

**Länsstyrelserna:** Swedish County Administrative Boards, in charge of the monitoring of large carnivores at the county level.

**MCMC:** Markov chain Monte Carlo.

**NGS:** Non-invasive genetic sampling.

**OPSCR:** Open-population spatial capture-recapture

**$p_0$ :** Baseline detection probability; probability of detecting an individual at a given detector, if the individual's AC is located exactly at the detector location.

**$\sigma$ :** Scale parameter of the detection function; related to the size of the circular home-range.

**SCR:** Spatial capture-recapture.

**SNO:** Statens naturoppsyn (Norwegian Nature Inspectorate) is the operative field branch of the Norwegian Environment Directorate (Miljødirektoratet).

**RovQuant:** Research group at the Norwegian University of Life Sciences (Ås, Norway) that develops and applies OPSCR models.

## 2 Methods

### 2.1 Data

We included data from multiple sources, the primary one being the Scandinavian large carnivore database Rovbase 3.0 (rovbase.se and rovbase.no; last extraction: 2023-10-20). This database is used jointly by Norway and Sweden to record detailed information associated with large carnivore monitoring, including, but not limited to, NGS data, dead recoveries, and GPS search tracks. In the following sections, we describe the various types of data used in the analysis. We used data collected during ten consecutive monitoring seasons from 2014 to 2023.

**Non-invasive genetic sampling** In Norway, the collection of wolverine scat, urine, glandular secretion, and hair is managed at the level of counties by SNO. Sample collection is conducted by SNO field officers, wardens at Statskog Fjelltjenesten (statskog.no), wardens at Fjellstyrene (fjellstyrene.no), local predator contacts, hunters and other members of the public. Rovdata (rovdata.no), a unit within the Norwegian Institute for Nature Research, has responsibility for the Norwegian large carnivore monitoring program. In Sweden, the collection of scat and hair is managed by Länsstyrelserna at the regional level and carried out by field officers from Länsstyrelserna. NGS collection was conducted primarily between December 1 and June 30 each year. NGS data collected late in the monitoring season and suspected to be from cubs were not included. This means that we only retained samples from individuals that were one year or older. DNA was isolated with an extraction robot (Maxwell 16, KingFisher or QIA Symphony instrument) and the samples were genotyped using 96 SNPs (Single Nucleotide Polymorphism) on a microfluidic-based platform (Biomark X9 instrument) for sex determination and individual identification. For further details on the DNA analysis procedure see Flagstad et al. (2004), Flagstad et al. (2021), and Kleven et al. (2023).

**Dead recoveries** In Scandinavia, all large carnivores killed legally (e.g., legal hunting, management kills, defense of life and property) have to be reported to the state authorities (Fylkesmannen or SNO in Norway and Länsstyrelserna or the police in Sweden). All wolverines found dead due to other reasons (e.g., natural deaths, vehicle and train collisions, illegal hunting) also have to be reported, but an unknown proportion remains undetected. Tissue is collected from all reported dead carnivores for DNA extraction and analysis, following the same procedures as for non-invasive genetic samples.

**GPS search tracks** Government employees involved in systematic searches for wolverine DNA following wolverine tracks (via snowmobiles, skis, snowshoes, etc.) document their effort with GPS track logs, which are registered in Rovbase 3.0. GPS search tracks were included in the OPSCR model to account for spatial and temporal variation in search effort during NGS.

**Observation reports in Skandobs** We used all observation records in the Skandobs database that were recorded during the wolverine monitoring seasons since 2012 (skandobs.se, skandobs.no; last extraction: 2023-10-24). Skandobs is a web application that allows anyone to anonymously register observations (visual, tracks, feces, etc.) of bears, lynx (*Lynx lynx*), wolves, and wolverines in Scandinavia. This data currently consists of more than 90 000 records of possible large carnivore observations. Although most observations are not verified, they offer the best available proxy for spatio-temporal variation in opportunistic effort at this time.



## 2.2 Open-population spatial capture-recapture model

We analysed the data using a Bayesian open-population spatial capture-recapture (OPSCR) model (Bischof et al., 2019b), which addresses three challenges associated with population-level wildlife inventories:

1. Detection is imperfect and sampling effort is heterogeneous in space and time: not all individuals present in the study area are detected (Kéry and Schaub, 2012).
2. Individuals that reside primarily outside the surveyed area may be detected within it. Without an explicit link between the population size parameter and the geographic area the population occupies, density cannot be estimated and population size is ill-defined (Efford, 2004).
3. Non-spatial population dynamic models usually estimate “apparent” survival and recruitment, as these parameters include the probability of permanent emigration and immigration, respectively. By explicitly modelling movement of individuals between years, the OPSCR model can help return unbiased estimates of demographic parameters (Ergon and Gardner, 2014; Schaub and Royle, 2014; Gardner et al., 2018).

The OPSCR model is composed of three sub-models:

1. A model for population dynamics and population size.
2. A model for density and individual movement.
3. A model for detections during DNA searches.

**Population dynamics and population size sub-model** We used a multi-state formulation (Lebreton and Pradel, 2002), where each individual’s life history is represented by a succession of up to 3 discrete states: (1) “unborn” if the individual has not yet been recruited into the population (state “unborn” is required for the data augmentation procedure, see below); (2) “alive” if it is alive; (3) “dead” if it is dead. We then modelled the transition from one state to another between consecutive monitoring seasons ( $t$  to  $t + 1$ ) to estimate vital rates (recruitment and mortality). More details are available in Bischof et al. (2019b) and Bischof et al. (2020b). This formulation of the population dynamic model means that, contrary to previous analyses (Bischof et al., 2019b, 2020b; Flagstad et al., 2021; Milleret et al., 2022b), we did not use dead recoveries or model cause-specific mortality directly in the OPSCR model. Cause-specific mortality was instead derived after model fitting (see section “Other derived parameters”). We used data augmentation (Royle and Dorazio, 2012), whereby additional, undetected individuals are available for inclusion in the population at each time step.

**Density and movement sub-model** We used a Bernoulli point process to model the distribution of individual ACs (Zhang et al., 2022). In the first year, individuals were located according to an intensity surface, which was a function of the locations of known dens at time  $t - 1$  (see Bischof et al., 2019b and Bischof et al., 2020b for more details). For all subsequent years ( $t > 1$ ), the location of individual ACs was a function of the distance from previous locations of ACs (at time  $t - 1$ ) and the locations of known wolverine dens (at time  $t - 1$ ). Similar to the wolf abundance estimation by Milleret et al. (2022d), we used an exponential model to describe the movement of individuals between years, as it better accommodates distributions with long tails (i.e., a few individuals that make exceptionally long dispersal movements).

**Detection sub-model** SCR models take into account the spatial variation in individual detection probability based on the distance between AC locations (estimated by the density sub-model) and a given detector. A half-normal function was used to express the declining probability of detection with increasing distance between the AC and the detector (Royle et al., 2013).

In Scandinavia, DNA material from live wolverines is collected following two main processes. First, authorities collect genetic samples and record the corresponding search effort during official searches ("structured sampling" thereafter). Second, DNA material can be collected by any member of the public (e.g., hunters) or by the authorities in a more or less opportunistic manner, which means that search effort is not directly available ("unstructured sampling" thereafter). Currently, it is not possible to unambiguously distinguish between samples collected by the authorities during the structured or unstructured sampling in Rovbase. We therefore assigned each sample to structured or unstructured sampling based on whether a given sample matched in time and space with recorded search tracks: a sample was assigned to the "structured" sampling if it was collected by the authorities (marked as collected by "Statsforvalteren" or "SNO" in Rovbase) and located within 500 m from a GPS search track recorded the same day. All remaining samples were assigned to the unstructured sampling.

We assumed that both sampling processes could in theory occur within the entire study area and therefore used the same  $10 \times 10$  km detector grid for both observation processes. Samples were then assigned to the closest detector (see details in Bischof et al., 2019b, and Bischof et al., 2020b). However, spatial and temporal variation in the probability to detect a sample during structured or unstructured sampling were assumed to be driven by different processes.

We accounted for spatial, temporal and individual heterogeneity in detectability during *structured sampling* using:

- Spatio-temporal variation in search effort represented by the length of GPS search tracks in each detector grid cell.
- Spatio-temporal variation in snow cover during the monitoring period calculated as the average percentage of snow cover in each detector grid cell (MODIS at 0.1 degrees resolution, <https://cmr.earthdata.nasa.gov>, accessed 2023-10-20).
- Spatio-temporal variation in monitoring regimes between jurisdictions (groups of counties in Sweden, carnivore management regions in Norway, Figure A.4).
- Individual variation linked with a detection during the previous occasion (monitoring season) that could be expected to influence the probability of being detected at the next occasion.

We accounted for spatial, temporal, and individual heterogeneity in detectability during *unstructured sampling* using:

- Spatio-temporal distribution of ancillary samples and samples not successfully genotyped (Figure A.1). For each detector grid cell and during each monitoring season (Dec 1 - Jun 30), we identified whether a) any carnivore sample had been registered in Rovbase (excluding successfully genotyped wolverine samples already used in the OPSCR analysis) or b) any observation of carnivores had been registered in Skandobs. Roughly, this binary variable distinguishes areas with very low detection probability from those with a higher probability that carnivore DNA samples, if present in a detector grid cell, could have been detected and submitted for genetic analysis (Figure A.1).
- Spatio-temporal variation in snow cover during the monitoring period calculated as the average percentage of snow cover in each detector grid cell (MODIS at 0.1 degrees resolution, <https://cmr.earthdata.nasa.gov>, accessed 2023-09-29).
- Spatial variation in accessibility measured as the average distance to the nearest road.

- Spatio-temporal variation between countries (Figure A.5).
- Individual and temporal variation linked with a previous detection that could influence the probability of being detected at subsequent occasions.

For years and areas without comprehensive sampling effort (i.e., Norrbotten county in Sweden in all years except 2017, 2018, and 2019), we removed all samples collected within the county and fixed detection probability to 0 for both structured and unstructured sampling. The different model components and data sources for covariates are described in detail in Bischof et al. (2019a), Bischof et al. (2019b), and Bischof et al. (2020b).

**Model fitting** We fitted sex-specific Bayesian OPSCR models using MCMC simulation with NIMBLE version 0.12.2 (de Valpine et al., 2017; Turek et al., 2021; de Valpine et al., 2022) and RovQuant’s R package nimbleSCR version 0.2.0 (Bischof et al., 2021) in R version 4.1.0 (R Core Team, 2021). We ran 4 chains each with 25 000 iterations, including a 10 000-iterations burn-in period. Due to the computing challenge associated with post-processing large amounts of data, we thinned chains by a factor of 10 before deriving abundance estimates. We considered models as converged when the Gelman-Rubin diagnostics (Rhat, Gelman and Rubin, 1992) was  $\leq 1.1$  for all parameters and when mixing between chains was satisfactory based on visual inspection of trace plots.

**Abundance estimates** To obtain an estimate of abundance for any given area, we summed the number of predicted AC locations (individuals detected during sampling or predicted to be alive by the model) that fell within that area for each iteration of the MCMC chains. This produced a posterior distribution of abundance for that area. From such posteriors, abundance estimates and the associated uncertainty can be extracted for any spatial unit, including countries, counties or management regions (Figure A.2). Individuals detected near a border can have their model-predicted AC placed on different sides of that border in different model iterations (even if detections are only made on one side of the border). As a result, the probability of designating such individuals to either side of the border can be integrated into jurisdiction-specific abundance estimates. This is especially relevant for wolverines detected along the Swedish and Norwegian border as individual wolverines can be partially designated to both countries (Bischof, 2015; Bischof et al., 2016).

To ensure that abundance estimates for spatial sub-units (jurisdictions) add up to the overall abundance estimate, we used the mean and associated 95% credible interval limits to summarize posterior distributions of abundance. Combined (female and male) parameter estimates were obtained by merging posterior samples from the sex-specific models.

**Density maps** We used both the distribution of model-estimated AC positions and the scale parameter ( $\sigma$ ) of the detection function to construct density maps based on individual utilization distributions. These maps are not only based on the position of the activity center of an individual, but also take into account the area over which that individual’s activity is spread, i.e., its space use (Bischof et al., 2020b). To do so, we constructed raster maps (5 km resolution) of individual utilization distributions, scaled values in each raster to sum to one, and then summed rasters across individuals to create a single population-level raster map for each iteration. An overall density map was derived by calculating the mean across iterations in each cell (Bischof et al., 2020b). Note that this approach assumes circular home ranges of average size for all individuals of a given sex and does not take into account individual variation in home-range size and shape.

**Other derived parameters** We did not use dead recoveries and did not model cause-specific mortalities explicitly. Instead, we used the posterior distribution of the number of individuals

that died between consecutive occasions, as estimated by the OPSCR model, and the recorded number of legally culled individuals to derive cause-specific mortality estimates indirectly.

The average proportion of individuals detected and the associated uncertainty were obtained by dividing the number of individuals detected through NGS each year (Table A.2) by the corresponding mean abundance estimates and associated credible interval limits, respectively.

We derived the proportion of females in the population and the associated uncertainty by dividing the estimated number of females by the total abundance for each iteration, thus generating a posterior distribution of the proportion of females from which the median and credible interval could be derived (Table A.2). Yearly population growth rates ( $\lambda$ ; Table A.5) were calculated similarly as  $\lambda_t = N_{t+1}/N_t$  for each iteration of the MCMC chains.

**Focus on uncertainty** Although we reported median (or mean for abundance; see above) estimates for all parameters in the tables, we intentionally focused the main results of our report on the 95% credible interval limits of the estimates. We did so with the aim of drawing the reader's attention to the uncertainty around population size estimates, rather than a single point estimate (Milleret et al., 2022b).

### 3 Results

#### 3.1 Non-invasive genetic samples and dead recoveries

A total of 21 746 (9 732 female; 12 014 male) genotyped wolverine genetic samples were included in the analysis, of which 42% originated from Sweden. These samples were associated with 2 830 (1500 female; 1330 male) individuals. We did not include individuals with unknown sex in this analysis. During the last sampling period (winter 2022/23), a total of 3 038 (1 358 female; 1 680 male) were successfully genotyped. Among all genotyped samples, 16 061 (7175 female; 8886 male) were assigned to structured sampling and 5 685 (2557 female; 3128 male) to unstructured sampling. Annual total and country-specific tallies of detections and associated individuals, as well as dead recoveries are provided in the appendices (NGS samples: Table A.1, number of individuals detected: Table A.2, number of dead recoveries: Table A.3)

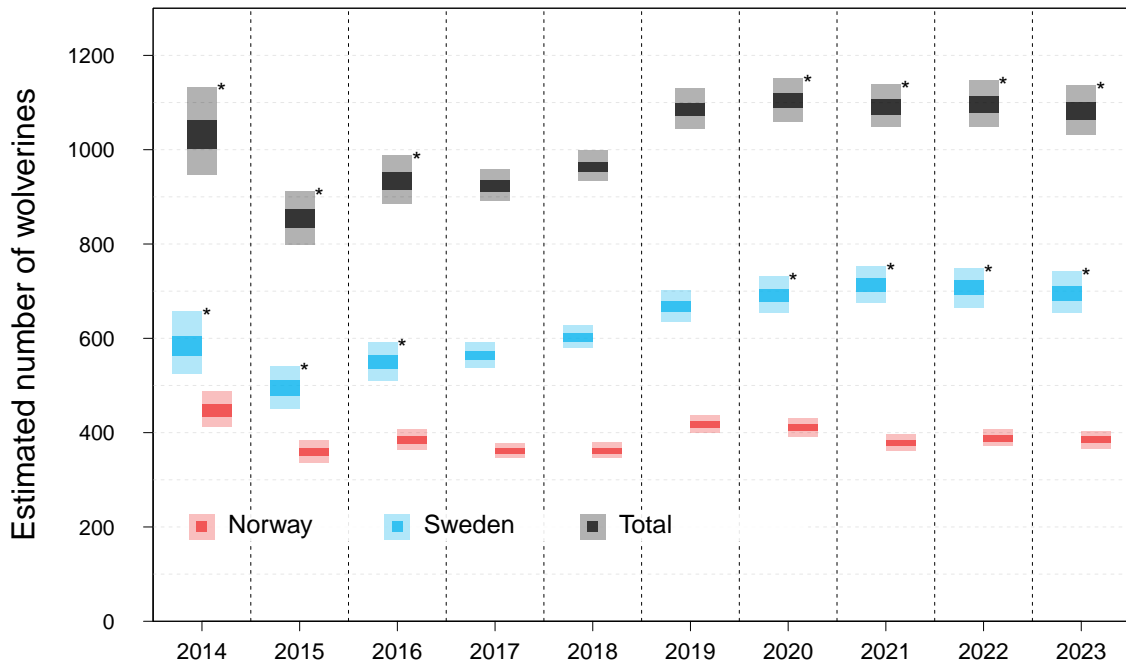


**Figure 1:** Total (black) and country-specific (blue: Sweden, red: Norway) annual wolverine population size estimates in Scandinavia between 2014 and 2023. Darker and lighter bars show the 50% and 95% credible intervals, respectively. Credible intervals indicate uncertainty in estimates given the model and data used to generate the estimates. Changes in the model and data can result in different estimates and associated uncertainty compared with estimates provided in previous reports by RovQuant. Total estimates in Sweden and for the entire study area that include estimates from Norrbotten without comprehensive NGS are marked with \*.

#### 3.2 Density and abundance

Wolverine abundance for the entire study area (622 350 km<sup>2</sup>, excluding the buffer area) was likely (95% credible interval) between 1 029 and 1 137 individuals in 2023 (Table 1, Figure 1, Figure 2). Estimates refer to the status of the population at the start of the annual sampling period (December 1). The proportion of females in the Scandinavian wolverine population was likely between 56% and 61% in 2023. Based on the model-predicted location of ACs, we estimated that in 2023, between 652 and 742 individuals could be attributed to Sweden and 366 to 403 to Norway. See Table 1 for total and sex-specific estimates for each country and carnivore management region. See Table A.4 for annual estimates for all of Scandinavia and by region between 2014 and 2023. Note that estimates for different years (Figure 1) shown here differ

slightly from those provided in Bischof et al. (2020b) and Milleret et al. (2021a). This is due to the use of an updated OPSCR model and the inclusion of an additional year of data. The analysis yielded annual density maps, which illustrate changes in the distribution of wolverines over time (Figure A.3).

**Table 1:** Wolverine population size estimates in 2023 by sex at several spatial scales: the entire study area, by country, by management unit (carnivore management regions in Norway and "Rovdjursförvaltningsområden" in Sweden), and by counties ("Län" in Sweden); see Figure A.2 for a labelled map. Only counties and management units that are within or that intersect the study area are included in the table. The percentage of the total area of each unit included in the analysis is provided in the column "% Area". Readers should focus on the 95% credible interval provided in parentheses, as these - unlike mean values - convey uncertainty inherent in abundance estimates. Numbers are based on estimated AC locations of wolverines. Combined female-male estimates were obtained by joining sex-specific posterior distributions. Rounding may result in small deviations between total estimates and the sum of the estimates for constituent regions. Estimates for Norrbotten county in years without comprehensive non-invasive genetic sampling (NGS) were derived solely using the prediction from the OPSCR model (shown in grey and marked with \*), without use of NGS data from that county. Total estimates in Sweden and for the entire study area that include estimates from Norrbotten without comprehensive NGS are shown in grey and marked with \*\*.

	Females	Males	Total	% Area
TOTAL	632.3 (586-680)**	448.6 (422-477)**	1081 (1029-1137)**	83
NORWAY	236.3 (221-253)	148.3 (139-159)	384.6 (366-403)	93
Region 1	7 (3-12)	4.5 (1-9)	11.6 (6-18)	85
Region 2	4 (1-8)	1.6 (0-4)	5.7 (2-10)	74
Region 3	18.2 (14-22)	14.4 (12-17)	32.6 (28-38)	100
Region 4	1 (0-3)	0.7 (0-3)	1.8 (0-5)	75
Region 5	44.7 (39-51)	36.5 (33-41)	81.2 (75-89)	100
Region 6	56.2 (50-63)	36.2 (32-41)	92.5 (84-101)	100
Region 7	43.2 (39-47)	28.8 (25-33)	72 (66-78)	100
Region 8	61.8 (55-70)	25.5 (22-30)	87.3 (79-96)	100
SWEDEN	396 (358-437)**	300.3 (276-325)**	696.4 (652-742)**	76
Norra	330.6 (297-368)**	235.7 (212-257)**	566.3 (527-609)**	100
Jämtland	121.5 (107-135)	87 (79-96)	208.5 (193-224)	100
Norrbotten*	111.2 (90-130)*	72.7 (55-91)*	183.8 (157-211)*	97
Västerbotten	71.3 (60-84)	50.6 (44-58)	121.8 (108-137)	97
Västernorrland	26.7 (20-34)	25.5 (21-30)	52.2 (44-61)	100
Mellersta	65.1 (56-76)	64.4 (56-74)	129.5 (117-143)	75
Dalarna	34.9 (30-41)	26.8 (23-32)	61.7 (55-69)	100
Gävleborg	17.7 (14-22)	22.1 (19-26)	39.8 (34-46)	100
Örebro	1.9 (0-5)	2.5 (0-6)	4.4 (1-9)	100
Stockholm	0.1 (0-1)	0.1 (0-1)	0.1 (0-1)	4
Uppsala	1.5 (0-4)	1.7 (0-4)	3.2 (0-7)	86
Värmland	7.3 (4-12)	9.6 (6-14)	16.9 (11-23)	100
Västmanland	0.9 (0-3)	0.9 (0-3)	1.7 (0-5)	74
VästraGötaland	0.8 (0-3)	0.7 (0-3)	1.6 (0-4)	12
Södra	0.3 (0-2)	0.3 (0-2)	0.6 (0-2)	1
Östergötland	0.2 (0-1)	0.1 (0-1)	0.3 (0-2)	4
Södermanland	0.2 (0-1)	0.1 (0-1)	0.3 (0-2)	7

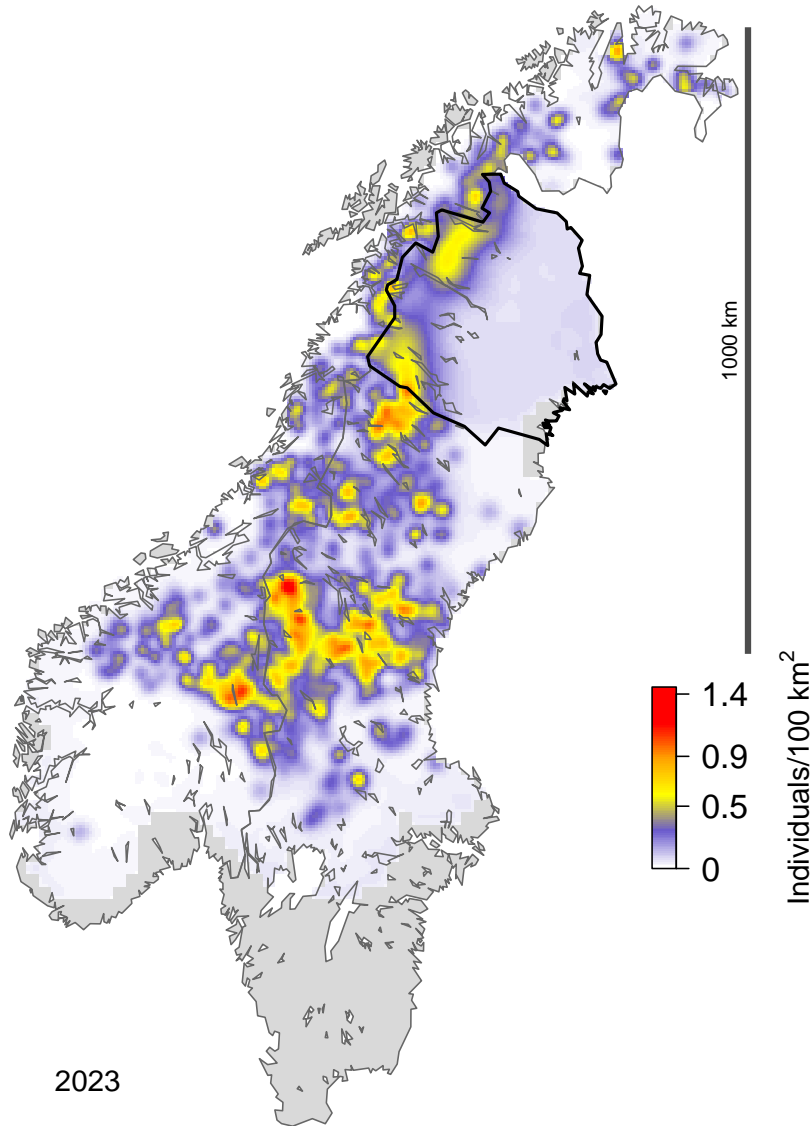


**Figure 2:** Wolverine density based on individual utilization distributions in Scandinavia in 2023. Note that no comprehensive NGS was conducted in Norrbotten (polygon outlined in black) in 2023, which means that the density estimated in this county is solely based on the OPSCR model prediction and assumptions. The grey background represents areas that were considered not searched and therefore were not included in the analysis. This map is freely available as a geo-referenced raster file at <https://github.com/richbi/RovQuantPublic>

### 3.3 Vital rates

The OPSCR model produced annual estimates of survival and per capita recruitment rates (Table A.6). Overall, females had a higher survival probability than males (Figure 3). Between 2022 and 2023, female wolverines experienced a significant apparent drop in survival (from 0.73-0.85 in 2022 to 0.58-0.71 in 2023, Table A.6). This drop did not seem to be caused by an increase in legal causes of mortality, but by an increase in mortality due to other causes (Figure 5). In 2023, the number of recruits was estimated to be between 316 and 429 (156-222 Females, 160-207 Males), which is higher than the number of recruits estimated in 2022 for both males and females (240-350; 108-176 Females, 132-174 Males; Figure 4).

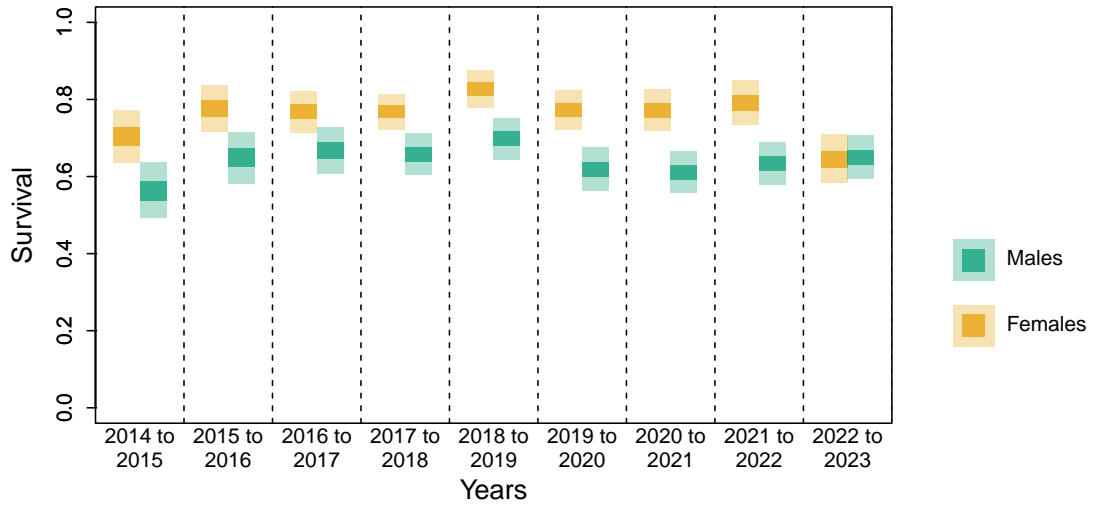


**Figure 3:** Annual survival probabilities for male and female wolverines. Darker and lighter bars show the 50% and 95% credible intervals, respectively. Shown are overall estimates for the entire study area between 2014 and 2023.

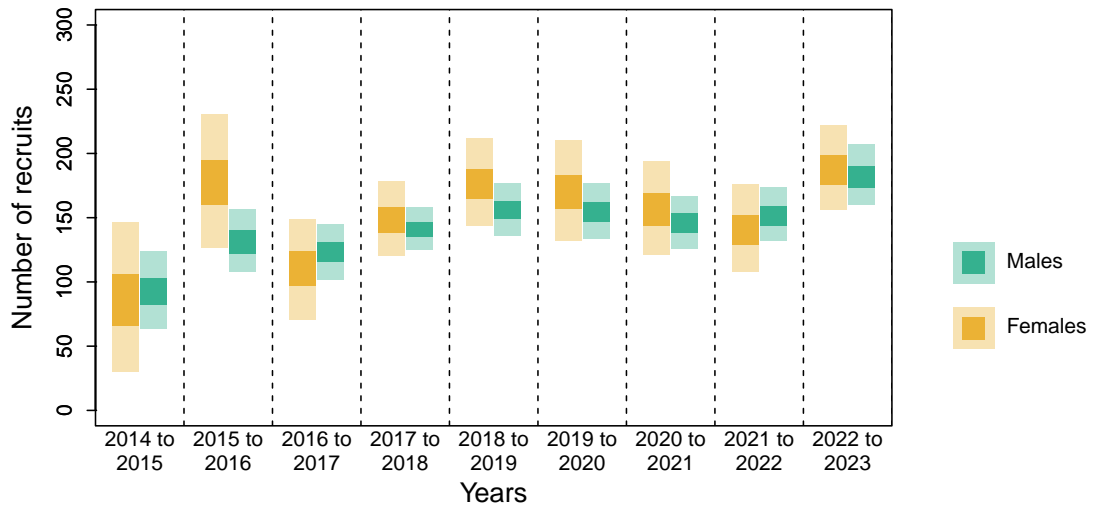


**Figure 4:** Estimated annual number of male and female recruits in the Scandinavian wolverine population between the start of one sampling season and the start of the next. Recruitment represents the number of new individuals present in the population on Dec 1 (i.e., individuals that were born between the two consecutive monitoring seasons and survived to Dec 1 or that immigrated into the study area). Darker and lighter bars show the 50% and 95% credible intervals, respectively.

### 3.4 Detection probability

The overall proportion of detected individuals in the population was likely between 65% and 71% in 2023, and overall, larger in Norway than in Sweden (Table A.10). The baseline detection probability for the structured and unstructured sampling varied both in time and space (Figure A.4 and Figure A.5). More specifically, the length of recorded search tracks positively



affected detection probability during structured sampling (2023; males:  $\beta = 0.46$ , CrI: 0.40 - 0.52; females:  $\beta = 0.51$ , CrI: 0.44 - 0.58; Table A.8). Detection of an individual during the previous year and the average proportion of snow cover had no significant effect on detection probability during structured sampling (Table A.8). The proxy for search effort during unstructured searches, derived using the observation data in Skandobs and information about ancillary samples in Rovbase, had a strong positive effect on detection probability during unstructured sampling (2023; males:  $\beta = 0.57$ , CrI: 0.31 - 0.84; females:  $\beta = 0.47$ , CrI: 0.15 - 0.81; Table A.9). Detection of an individual during the previous year also tended to have a positive effect on detection probability during unstructured sampling but the pattern was not consistent across years (Table A.9).

## 4 Discussion

The drop in the survival estimates of female wolverines between 2022 and 2023 was unexpected. Further analyses, that explicitly integrated spatial dead recoveries in the OPSCR model (Dupont et al., 2021; Bischof et al., 2020b; Milleret et al., 2021a), indicated that the drop was not due to an increase in legal mortality, but due to an increase in mortality due to other causes (Figure 5). Other causes of mortality include natural (e.g., age, diseases, starvation, intra- and interspecific killing), traffic and illegal killing, which we cannot differentiate, and remains undetected in most cases. With our present analysis, we were unable to identify the reason behind the apparent drop in female survival in the last year of the time series. We consider two main, non-mutually exclusive, explanations for this result:

1) A true reduction in survival due to one or more factors. An increase in other causes of mortality can be linked, for example, with an increase in natural mortality caused by intra-specific aggression (due to higher densities) or disease. Alternatively, anthropogenic factors could cause a spike in mortalities, for example an increase in illegal killing, or a combination thereof. However, we are not aware of any reports or observations that would support these hypotheses.

2) An analytical artifact. Such issue can arise with a mismatch between the observation and ecological process of the OPSCR model. For example, if the detection of females already alive in 2022 was lower in 2023 but not unaccounted for in the analysis, this could lead to an apparent decrease in survival. However, we are not aware of major changes in sample collection or genotyping procedures during wolverines monitoring between 2022 and 2023 in Sweden and Norway that could explain such differences in detectability. On the contrary, overall figures of detectability, as shown by the number of genotyped samples (Table A.1, Table A.2 ) and the estimated baseline detection probability (Figure A.4), seemed higher than previous years in Norway and rather stable in Sweden. We also cannot discard the possibility that the OPSCR approach inadvertently introduced a bias. Our analysis revealed a stable survival of males but a decrease in the survival of females between 2022-2023. The analysis also revealed a higher number of recruits from both sexes between 2022-2023. Finally, these patterns, including the higher number of recruits for both males and females, are also visible in the raw NGS data, which suggests that a bias caused by the OPSCR model is unlikely to be the main explanation for the decrease in survival.

Our analysis did not allow us to draw conclusions about one or more of these potential explanations as the cause of the observed pattern. Further analyses, such as a spatially explicit estimation of mortality (Milleret et al., 2022a), could help reveal if this decrease in female survival is homogeneous across Sweden and Norway and, ultimately, to identify whether it is real or an artifact.

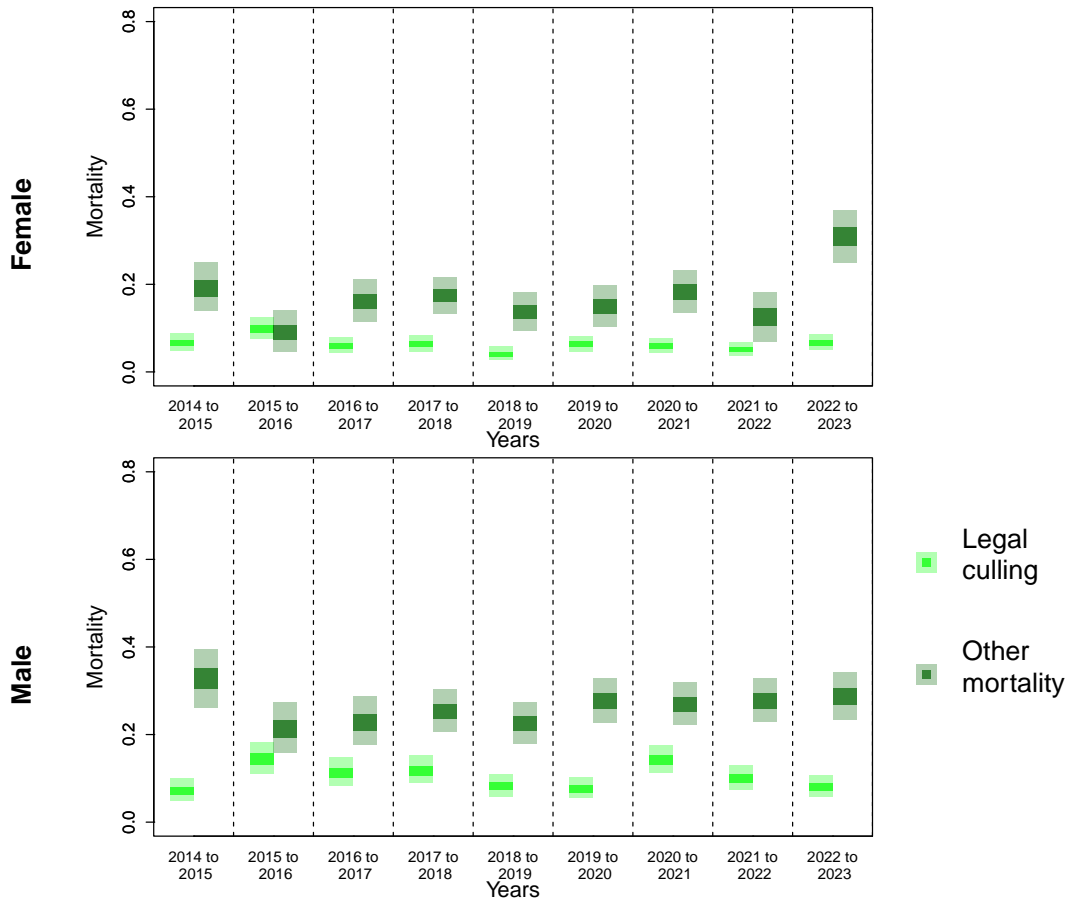


**Figure 5:** Mortality probabilities due to legal culling (light green) and all other causes (dark green) for female and male wolverines estimated by a separate OPSCR model that integrated dead recoveries (Dupont et al., 2021; Bischof et al., 2020b; Milleret et al., 2021a). Darker and lighter bars show the 50% and 95% credible intervals, respectively. Shown are overall estimates throughout the study area. Estimates refer to deaths occurring between the start of one sampling season and the start of the next.

## 5 Summary and suggestions of improvements

### 5.1 Summary of improvements made

The analysis described in this report includes the following adjustments compared with previous analyses of wolverine density in Scandinavia by RovQuant (Milleret et al., 2022c):

1. Addition of data from the 2023 monitoring season.
2. Correction of a previous error in the assignment of some samples to structured and unstructured sampling.

### 5.2 Suggestions for future improvements

RovQuant continues to work on improving the functionality and efficiency of OPSCR models. We plan to test and potentially implement the following developments in future analyses of the Scandinavian wolverine monitoring data:

1. Review and adjust spatial covariates on density. This may involve the addition of relevant spatial variables (Moqanaki et al., 2022).
2. Account for individual heterogeneity in detection for example by using a finite-mixture approach (Cubaynes et al., 2010).
3. Consider alternative detection models that do not assume a half-normal shape and/or circular home ranges (Sutherland et al., 2015; Dey et al., 2022).
4. Account for spatial variation in survival (Milleret et al., 2022a).

### 5.3 Other recommendations

In addition, we suggest the following:

1. Indicate sample association with the search tracks in Rovbase (if any) to unambiguously identify samples arising from structured vs unstructured sampling.
2. Consider full-coverage NGS in all regions for which estimates are desired (e.g., Norbotten or reindeer (*Rangifer tarandus*) herding areas).
3. Report information about how samples are selected for DNA analysis.
4. Record coarse measures of search conditions at the search track level (e.g., presence/absence of snow, days since last snowfall, experience level of searchers).
5. Unambiguously and consistently indicate the species targeted during searches when recording GPS search tracks.
6. Clearly identify and delineate areas excluded from structured and unstructured sampling and indicate the reason for exclusion (e.g., unable to search the area or low priority due to assumed absence of the target species).
7. Explore the feasibility of using station-based detectors (e.g., hair snares or similar) for better control over the observation process.

## 6 Acknowledgements

This work was made possible by the large carnivore monitoring programs and the extensive monitoring data collected by Swedish (Länstyrelsen) and Norwegian (SNO) wildlife management authorities, as well as the public in both countries. Our analyses relied on genetic analyses conducted by the laboratory personnel at the DNA laboratories at the Swedish University of Agricultural Sciences, and the Norwegian Institute for Nature Research. We also thank Swedish and Norwegian wildlife managers for feedback provided during project RovQuant. This work was funded by Naturvårdsverket (NV-366-23-005), Miljødirektoratet (22047026), and the Research Council of Norway (NFR 286886; project WildMap). Computation was performed on resources provided by NMBU's computing cluster Orion and by UNINETT Sigma2 - the National Infrastructure for High Performance Computing and Data Storage in Norway. We are grateful to P. de Valpine and D. Turek for help with the formulation of the OPSCR model in Nimble. J. Vermaat provided helpful comments on a draft of this report.

## 7 Data availability

Data, R code to reproduce the analysis, as well as figures, tables, and raster maps (Figure A.3) are available at <https://github.com/richbi/RovQuantPublic>.

## References

- Bischof, R. (2015). Approaches for assessing illegal hunting of brown bears and other large carnivores in Sweden. *Report 2015:5 from the Scandinavian Brown Bear Research Project to the Swedish Environmental Protection Agency. Norwegian University of Life Sciences, Ås, Norway.*
- Bischof, R., Brøseth, H., and Gimenez, O. (2016). Wildlife in a Politically Divided World: Insularism Inflates Estimates of Brown Bear Abundance. *Conservation Letters*, 9(2):122–130.
- Bischof, R., Dupont, P., Milleret, C., Chipperfield, J., and Royle, J. A. (2020a). Consequences of ignoring group association in spatial capture–recapture analysis. *Wildlife Biology*, 2020(1):1–10.
- Bischof, R., Milleret, C., Dupont, P., Chipperfield, J., Åkesson, M., Brøseth, H., and Kindberg, J. (2019a). Estimating the size of the Scandinavian wolf population with spatial capture recapture and conversion factors. *MINA fagrapport 57*, 80pp.
- Bischof, R., Milleret, C., Dupont, P., Chipperfield, J., Brøseth, H., and Kindberg, J. (2019b). Estimating density, abundance and population dynamics of bears, wolverines, and wolves in Scandinavia. *MINA fagrapport 63*, 79pp.
- Bischof, R., Milleret, C., Dupont, P., Chipperfield, J., Tourani, M., Ordiz, A., de Valpine, P., Turek, D., Royle, J. A., Gimenez, O., Flagstad, O., Åkesson, M., Svensson, L., Brøseth, H., and Kindberg, J. (2020b). Estimating and forecasting spatial population dynamics of apex predators using transnational genetic monitoring. *Proceedings of the National Academy of Sciences*, 117(48):30531–30538.
- Bischof, R., Turek, D., Milleret, C., Ergon, T., Dupont, P., Dey, S., and de Valpine, P. (2021). *nimbleSCR: Spatial Capture-Recapture (SCR) Methods Using 'nimble'*. R package version 0.1.2.
- Chandler, R. B., Hepinstall-Cymerman, J., Merker, S., Abernathy-Conners, H., and Cooper, R. J. (2018). Characterizing spatio-temporal variation in survival and recruitment with integrated population models. *The Auk*, 135(3):409–426.
- Cubaynes, S., Pradel, R., Choquet, R., Duchamp, C., Gaillard, J. M., Lebreton, J. D., Marboutin, E., Miquel, C., Reboulet, A. M., Poillot, C., Taberlet, P., and Gimenez, O. (2010). Importance of accounting for detection heterogeneity when estimating abundance: the case of French wolves. *Conservation Biology*, 24(2):621–626.
- de Valpine, P., Paciorek, C., Turek, D., Michaud, N., Anderson-Bergman, C., Obermeyer, F., Wehrhahn Cortes, C., Rodríguez, A., Temple Lang, D., and Paganin, S. (2022). *NIMBLE User Manual*. R package manual version 0.12.2.
- de Valpine, P., Turek, D., Paciorek, C. J., Anderson-Bergman, C., Lang, D. T., and Bodik, R. (2017). Programming with models: writing statistical algorithms for general model structures with NIMBLE. *Journal of Computational and Graphical Statistics*, 26(2):403–413.
- Dey, S., Bischof, R., Dupont, P. P. A., and Milleret, C. (2022). Does the punishment fit the crime? consequences and diagnosis of misspecified detection functions in Bayesian spatial capture–recapture modeling. *Ecology and Evolution*, 12(2):e8600.
- Dupont, P., Milleret, C., Brøseth, H., Kindberg, J., and Bischof, R. (2022). Estimates of brown bear density, abundance, and population dynamics in norway 2012 - 2021. *MINA fagrapport 82*, 32pp.
- Dupont, P., Milleret, C., Brøseth, H., Kindberg, J., and Bischof, R. (2023). Estimates of brown bear density, abundance, and population dynamics in norway 2012 - 2022. *MINA fagrapport 86*, 33pp.
- Dupont, P., Milleret, C., Tourani, M., Brøseth, H., and Bischof, R. (2021). Integrating dead recoveries in open-population spatial capture–recapture models. *Ecosphere*, 12(7):e03571.
- Efford, M. (2004). Density estimation in live-trapping studies. *Oikos*, 106(3):598–610.
- Ergon, T. and Gardner, B. (2014). Separating mortality and emigration: modelling space use, dispersal and survival with robust-design spatial capture–recapture data. *Methods in Ecology and Evolution*, 5(12):1327–1336.
- Flagstad, Ø., Hedmark, E., Landa, A., Brøseth, H., Persson, J., Andersen, R., Segerström, P., and Ellegren, H. (2004). Colonization history and noninvasive monitoring of a reestablished wolverine population. *Conservation Biology*, 18(3):676–688.
- Flagstad, Ø., Kleven, O., Brandsegg, H., Spets, M., Eriksen, L., Andersskog, I., Johansson, M., Ekblom, R., Ellegren, H., and Brøseth, H. (2021). DNA-basert overvåking av den skandinaviske jervebestanden 2020. *Norsk institutt for naturforskning(NINA), Trondheim, NINA Rapport nr 1956.*
- Gardner, B., Sollmann, R., Kumar, N. S., Jathanna, D., and Karanth, K. U. (2018). State space and movement specification in open population spatial capture–recapture models. *Ecology and Evolution*, 8(20):10336–10344.
- Gelman, A. and Rubin, D. (1992). Inference from iterative simulation using multiple sequences. *Statistical Science*, 7:457–511. <http://www.stat.columbia.edu/~gelman/research/published/itsim.pdf>.
- Kéry, M. and Schaub, M. (2012). *Bayesian population analysis using WinBUGS: a hierarchical perspective*. Academic Press, Waltham, MA.
- Kleven, O., Spets, M. H., Königsson, H., Spong, G., Milleret, C., Dupont, P., Bischof, R., and Brøseth, H. (2023). DNA-basert overvåking av den skandinaviske jervebestanden 2023. *Norsk institutt for naturforskning*.

- ing(NINA), Trondheim*, NINA Rapport nr 2386.
- Lebreton, J.-D. and Pradel, R. (2002). Multistate recapture models: modelling incomplete individual histories. *Journal of Applied Statistics*, 29:353–369.
- Milleret, C., Bischof, R., Dupont, P., Brøeth, H., Odden, J., and Mattisson, J. (2021a). GPS collars have an apparent positive effect on the survival of a large carnivore. *Biology Letters*, 17(6):20210128.
- Milleret, C., Dey, S., Dupont, P., Brøseth, H., Turek, D., de Valpine, P., and Bischof, R. (2022a). Estimating spatially variable and density-dependent survival using open-population spatial capture–recapture models. *Ecology*, n/a(n/a):e3934. e3934 ECY22-0819.
- Milleret, C., Dupont, P., Bonenfant, C., Brøseth, H., Flagstad, O., Sutherland, C., and Bischof, R. (2019). A local evaluation of the individual state-space to scale up Bayesian spatial capture recapture. *Ecology and Evolution*, 9(1):352–363.
- Milleret, C., Dupont, P., Brøseth, H., Flagstad, O., Kindberg, J., and Bischof, R. (2022b). Estimates of wolverine density, abundance, and population dynamics in Scandinavia, 2013–2021. *MINAfaagrapport 74*, 30pp.
- Milleret, C., Dupont, P., Brøseth, H., Flagstad, O., Kindberg, J., Svensson, L., and Bischof, R. (2023). Estimates of wolf density, abundance, and population dynamics in Scandinavia, 2013–2023. *MINAfaagrapport 85*, 34pp.
- Milleret, C., Dupont, P., Brøseth, H., Kindberg, J., Royle, J. A., and Bischof, R. (2018). Using partial aggregation in spatial capture recapture. *Methods in Ecology and Evolution*, 9(8):1896–1907.
- Milleret, C., Dupont, P., Moqanaki, E., Brøseth, H., Flagstad, O., Kleven, O., Kindberg, J., and Bischof, R. (2022c). Estimates of wolverine density, abundance, and population dynamics in Scandinavia, 2014–2022. *MINAfaagrapport 79*, 35pp.
- Milleret, C., Dupont, P., Åkesson, M., Brøseth, H., Kindberg, J., and Bischof, R. (2021b). Estimates of wolf density, abundance, and population dynamics in Scandinavia, 2012 - 2021. *MINAfaagrapport 72*, 30pp.
- Milleret, C., Dupont, P., Åkesson, M., Svensson, L., Brøseth, H., Kindberg, J., and Bischof, R. (2022d). Estimates of wolf density, abundance, and population dynamics in Scandinavia, 2013–2022. *MINAfaagrapport 77*, 35pp.
- Moqanaki, E., Milleret, C., Dupont, P., Brøseth, H., and Bischof, R. (2022). Wolverine density distribution reflects past persecution and current management in Scandinavia. *bioRxiv*.
- R Core Team (2021). *R: A Language and Environment for Statistical Computing*. R Foundation for Statistical Computing, Vienna, Austria.
- Royle, J. A., Chandler, R. B., Sollmann, R., and Gardner, B. (2013). *Spatial capture-recapture*. Elsevier/Academic Press, Amsterdam.
- Royle, J. A. and Dorazio, R. M. (2012). Parameter-expanded data augmentation for Bayesian analysis of capture–recapture models. *Journal of Ornithology*, 152(2):521–537.
- Schaub, M. and Royle, J. A. (2014). Estimating true instead of apparent survival using spatial Cormack–Jolly–Seber models. *Methods in Ecology and Evolution*, 5(12):1316–1326.
- Sutherland, C., Fuller, A. K., and Royle, J. A. (2015). Modelling non-Euclidean movement and landscape connectivity in highly structured ecological networks. *Methods in Ecology and Evolution*, 6(2):169–177.
- Turek, D., Milleret, C., Ergon, T., Brøseth, H., Dupont, P., Bischof, R., and de Valpine, P. (2021). Efficient estimation of large-scale spatial capture–recapture models. *Ecosphere*, 12(2):e03385.
- Zhang, W., Chipperfield, J. D., Illian, J. B., Dupont, P., Milleret, C., de Valpine, P., and Bischof, R. (2022). A flexible and efficient bayesian implementation of point process models for spatial capture-recapture data. *Ecology*, page e3887. e3887.

# Appendices

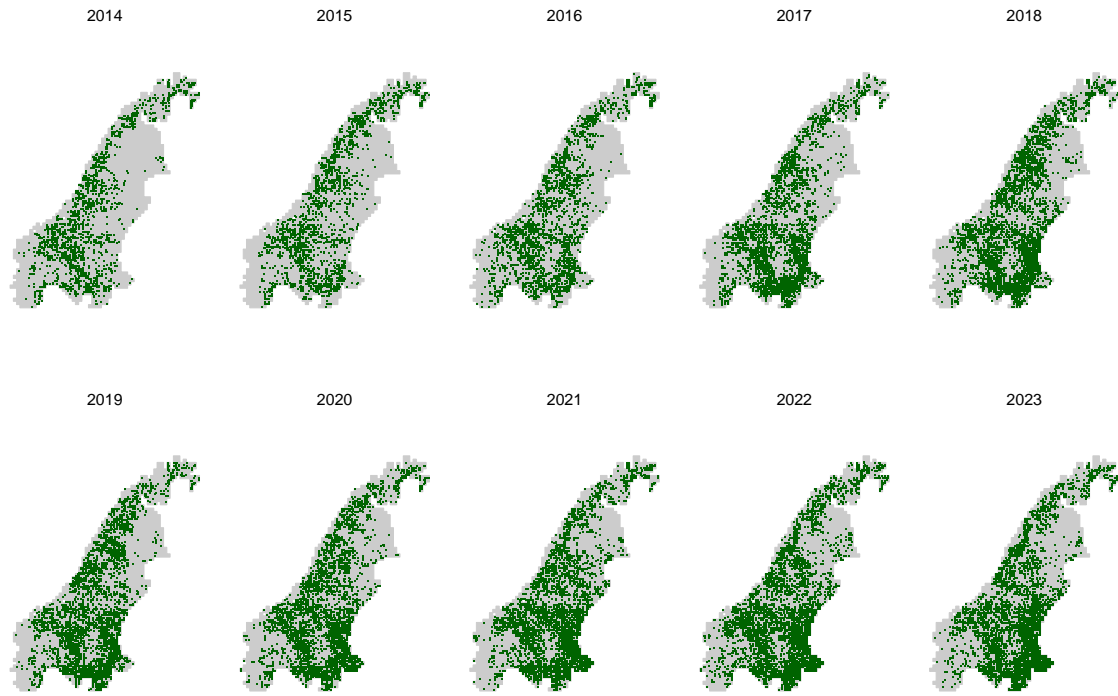


**Figure A.1:** Covariate used to account for spatio-temporal variation in unstructured sampling in the study area. Green cells ( $10 \times 10$  km) represent areas with at least one carnivore record from Rovbase (rovbase.no, rovbase.se, excluding the wolverine samples used in the OPSCR model) or an observation record from Skandobs (skandobs.se, skandobs.no) during a given monitoring season (Dec 1 – Jun 30).



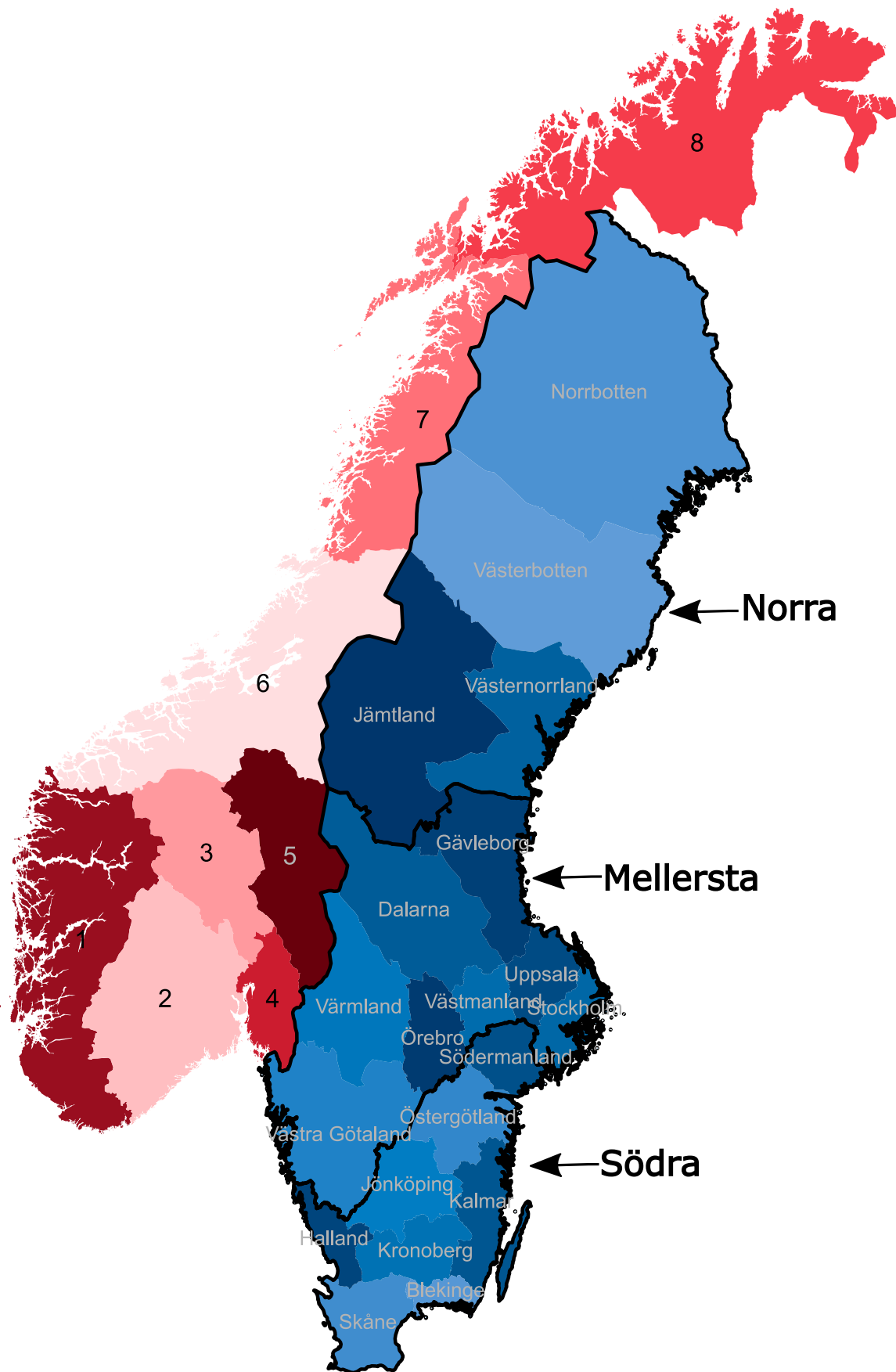


**Figure A.2:** Management jurisdictions in Norway and Sweden. Polygons with different shading represent carnivore management regions in Norway and counties in Sweden. Thick outlines delineate Swedish carnivore management regions ("Rovdjursförvaltningsområden") encompassing multiple counties.

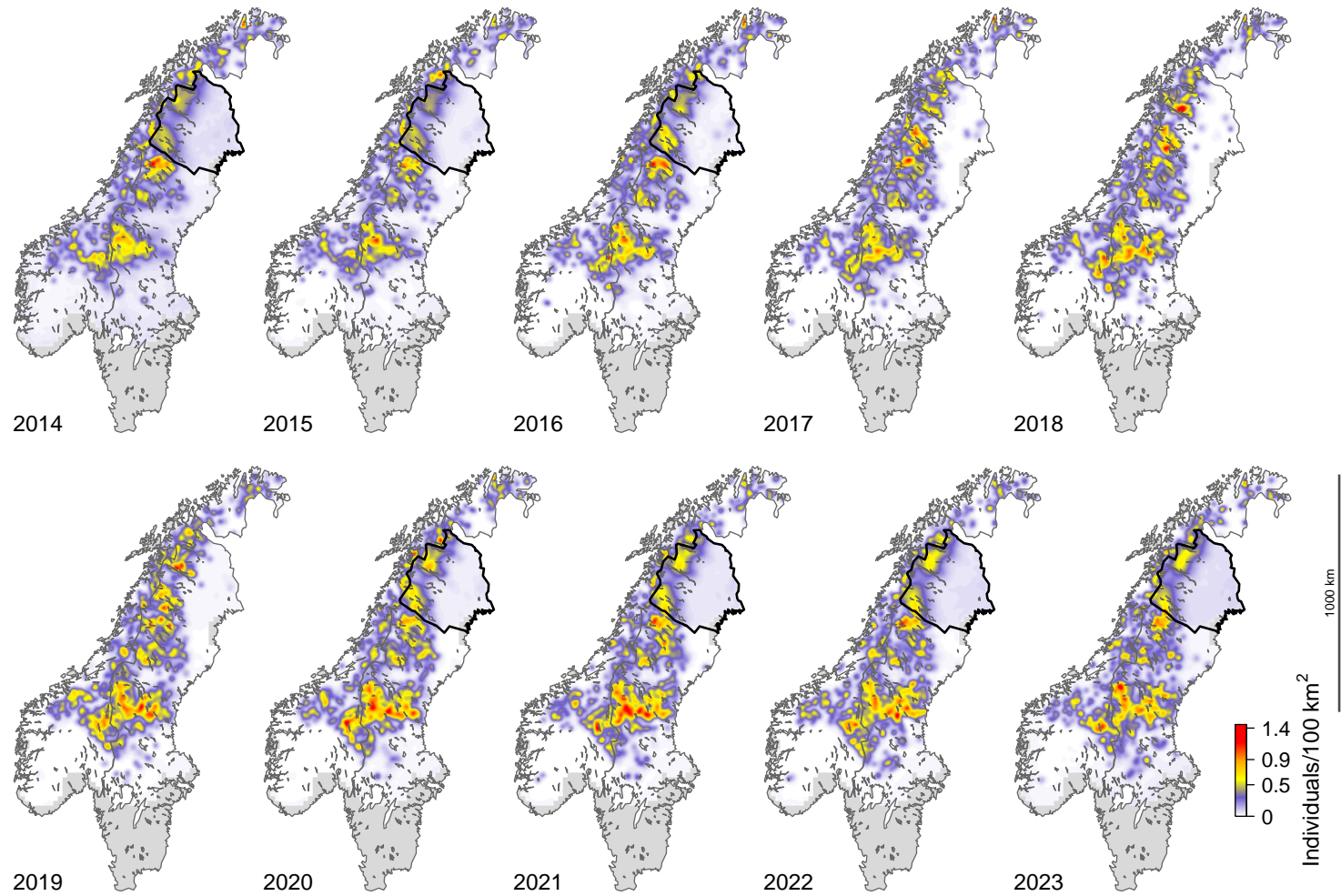


**Figure A.3:** Wolverine density based on individual utilization distributions in Scandinavia between 2014 and 2023. Note that no comprehensive NGS was conducted in Norrbotten (polygon outlined in black) from 2014-2016 and from 2020-2023, which means that the results are solely based on the OPSCR model prediction and assumptions. The grey area represents areas that were considered not searched and therefore were not included in the analysis. These maps are available as geo-referenced raster files at <https://github.com/richbi/RovQuantPublic>.

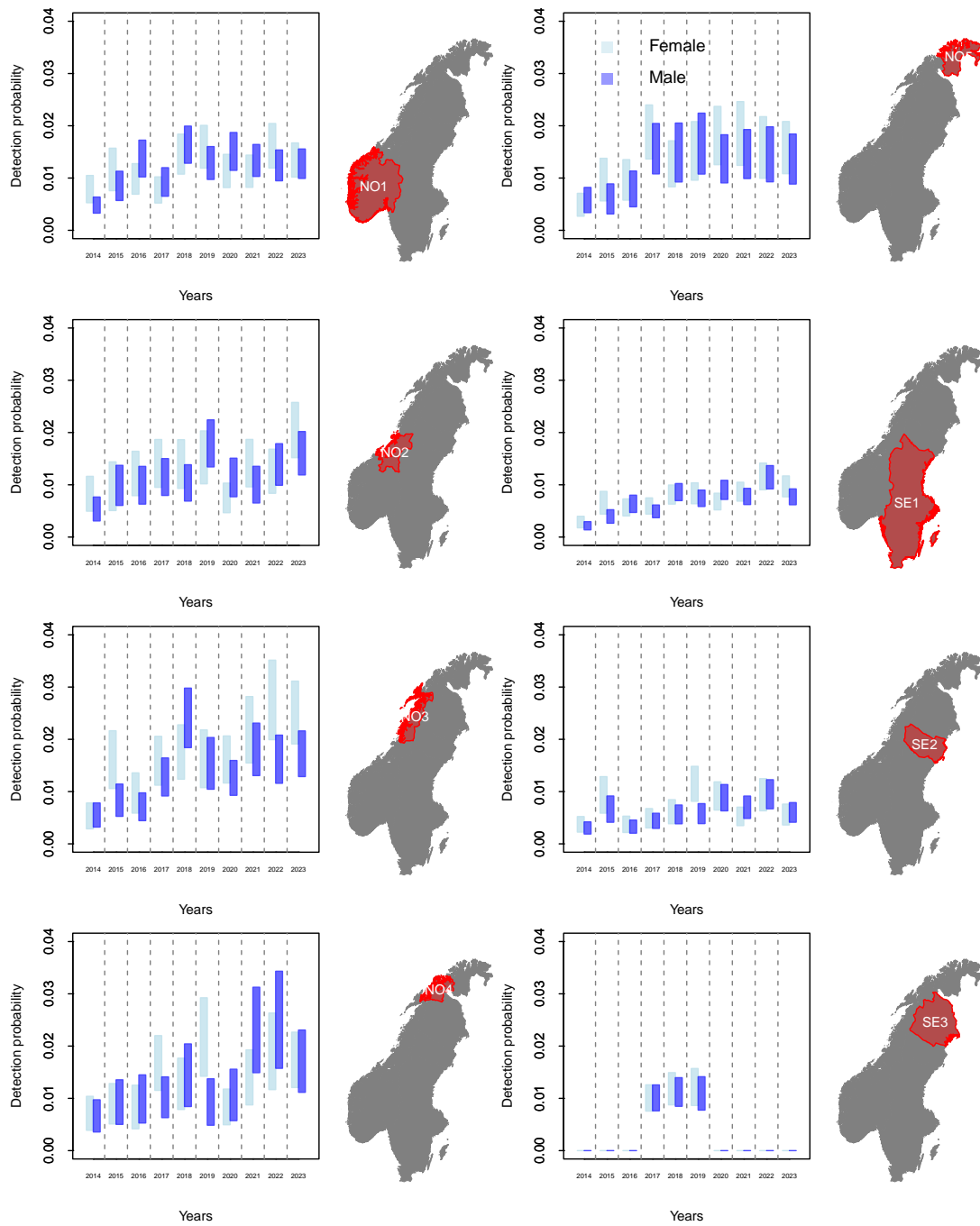


**Figure A.4:** Sex-specific baseline detection probabilities ( $p_{0,structured}$ ) for the different Scandinavian jurisdictions during structured sampling as estimated by the open-population spatial capture-recapture (OPSCR) model. Bars represent 95% credible intervals. Results are separated into panels based on regions. Estimates are shown for the mean values of the detection covariates. Note that baseline detection probability ( $p_0$ ) is a theoretical value of detection probability when a detector coincides with the location of an individual's AC; it is not to be confused with detectability, i.e., the overall probability of detecting an individual.

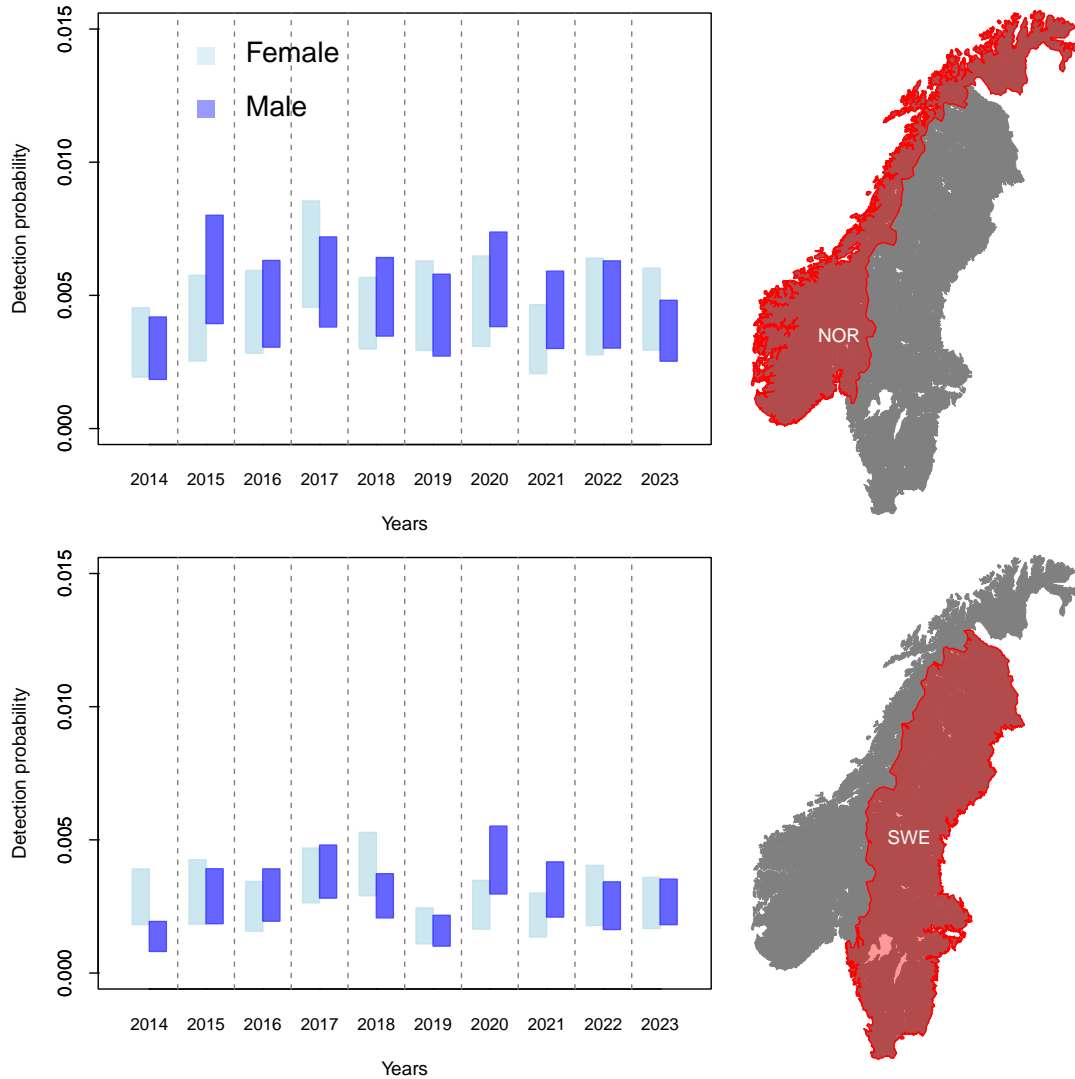


**Figure A.5:** Sex- and country-specific baseline detection probabilities ( $p_{0unstructured}$ ) of wolverines during unstructured sampling as estimated by the open-population spatial capture-recapture (OPSCR) model. Bars represent 95% credible intervals. Estimates are shown for the mean values of the detection covariates. Note that baseline detection probability ( $p_0$ ) is a theoretical value of detection probability when a detector coincides with the location of an individual's activity center; it is not to be confused with detectability, i.e., the overall probability of detecting an individual.

**Table A.1:** Annual number of wolverine non-invasive genetic samples included in the analysis. Numbers are reported by country, for females (F) and males (M), and for each type of sampling (structured and unstructured). We included only samples collected within the study area during the primary monitoring period (Dec 1 - June 30) between 2014 and 2023.

	2014		2015		2016		2017		2018		2019		2020		2021		2022		2023	
	F	M	F	M	F	M	F	M	F	M	F	M	F	M	F	M	F	M	F	M
Norway	521	578	412	445	470	577	606	670	462	747	592	731	575	686	582	736	569	747	877	999
Sweden	186	154	228	221	236	275	487	552	636	839	504	618	355	538	460	563	493	657	481	681
Total	707	732	640	666	706	852	1093	1222	1098	1586	1096	1349	930	1224	1042	1299	1062	1404	1358	1680

**Table A.2:** Annual number of individual wolverines detected via non-invasive genetic sampling and included in the analysis. Numbers are reported by country, for females (F) and males (M), and for each type of sampling (structured and unstructured). We included only individuals associated with samples collected within the study area during the primary monitoring period (Dec 1 - Jun 30) between 2013/2014 and 2021/2023. Some individuals were detected in both countries during the same year, hence the sum of the national counts can exceed the total number of unique individuals detected in Scandinavia.

	2014		2015		2016		2017		2018		2019		2020		2021		2022		2023	
	F	M	F	M	F	M	F	M	F	M	F	M	F	M	F	M	F	M	F	M
Norway	189	135	155	114	180	123	182	132	171	123	192	150	193	153	187	136	194	137	214	152
Sweden	85	70	106	86	107	105	211	177	231	211	225	197	172	156	207	167	194	180	193	194
Total	271	203	256	193	284	224	377	288	391	316	408	334	360	303	388	297	387	308	397	338

**Table A.3:** Number of cause-specific dead recoveries of wolverines in Scandinavia between 2014 and 2023. Numbers are reported by country, for females (F) and males (M). Dead recovery data was only used to derive cause-specific mortality and for the additional analysis presented in Figure 5

	Country	2014		2015		2016		2017		2018		2019		2020		2021		2022		2023	
		F	M	F	M	F	M	F	M	F	M	F	M	F	M	F	M	F	M	F	M
<b>Other</b>	Norway	42	37	67	53	44	43	50	62	32	31	55	36	54	60	45	46	43	45	38	40
	Sweden	1	3	1	2	0	2	0	1	1	2	1	1	0	1	2	1	6	5	6	10
<b>Legal culling</b>	Norway	1	3	2	1	1	1	0	1	2	1	3	4	0	6	3	2	0	0	0	0
	Sweden	13	8	22	18	6	9	5	2	1	5	6	3	7	19	3	10	8	1	5	2
<b>Total</b>	Total	57	51	92	74	51	55	55	66	36	39	65	44	61	86	53	59	57	51	49	52

**Table A.4:** Annual abundance estimates for wolverine at several spatial scales: the entire study area, by country, by management unit (carnivore management regions in Norway and "Rovdjursförvaltningsområden" in Sweden), and counties ("Län" in Sweden); see also Figure A.2. Only counties and management units that are within or that intersect the study area are included in the table. Estimates are based on model-estimated activity center locations. Credible intervals (95%) are shown in parentheses. Small deviations between the total estimate and the sum of abundance estimates from the constituent sub-regions may arise due to rounding. Note that the numbers reported here are predictions from a statistical model which always represents an oversimplification of reality and is based on available data (NGS). As a consequence, especially at the local scale, the model-estimated number of wolverines based on DNA sampling can deviate from the number of wolverines inferred from ancillary observations (e.g., camera traps). Estimates for Norrbotten county in years without comprehensive NGS were derived solely using the prediction from the OPSCR model (shown in grey and marked with \*). Total estimates in Sweden and for the entire study area that includes estimates from Norrbotten without comprehensive NGS are marked with \*\*.

	2014	2015	2016	2017	2018	2019	2020	2021	2022	2023
TOTAL	1032.2 (947-1134)**	854.1 (797-911)**	934.1 (885-988)**	923.7 (892-959)	964.5 (935-999)	1085.7 (1043-1131)	1103.4 (1059-1151)**	1091 (1047-1139)**	1096.1 (1046-1147)**	1081 (1029-1137)**
NORWAY	447.1 (413-488)	359.3 (337-385)	383.4 (362-406)	360.7 (345-377)	361.6 (347-380)	417.2 (399-437)	411.5 (392-431)	377.9 (361-397)	389 (371-408)	384.6 (366-403)
Region 1	22.1 (15-31)	11.7 (7-18)	10 (6-16)	8 (4-13)	6.4 (3-11)	6.4 (2-11)	6.1 (2-11)	6.9 (3-12)	10 (5-16)	11.6 (6-18)
Region 2	9.2 (4-16)	3.4 (0-8)	3.5 (1-7)	3.1 (1-6)	2.1 (0-5)	2.4 (0-6)	2.5 (0-6)	4.2 (1-8)	4.4 (1-9)	5.7 (2-10)
Region 3	37.8 (31-45)	27.7 (22-33)	27.1 (22-33)	23.7 (20-28)	22.4 (18-27)	27.8 (23-33)	30.4 (26-35)	32.3 (27-38)	27.4 (23-33)	32.6 (28-38)
Region 4	3.2 (0-7)	1.3 (0-4)	1.1 (0-3)	0.9 (0-3)	0.5 (0-2)	0.7 (0-3)	1 (0-3)	0.9 (0-3)	1 (0-3)	1.8 (0-5)
Region 5	67.4 (58-78)	56.1 (48-65)	65 (59-72)	65.2 (58-73)	77.5 (70-85)	93.9 (87-102)	92.4 (85-100)	87.5 (80-95)	90 (83-97)	81.2 (75-89)
Region 6	89.5 (77-102)	73.1 (64-83)	80.5 (71-90)	81.5 (74-89)	90.5 (82-99)	103.2 (94-112)	89.1 (79-99)	83.4 (75-92)	99.3 (91-108)	92.5 (84-101)
Region 7	80.1 (70-91)	71.3 (64-79)	83 (76-90)	69.9 (65-76)	67.4 (62-74)	78.9 (72-86)	88.8 (81-96)	69.5 (63-76)	68.2 (62-75)	72 (66-78)
Region 8	137.8 (124-152)	114.8 (105-126)	113.1 (103-123)	108.5 (102-116)	94.9 (88-103)	103.9 (96-113)	101.3 (94-110)	93.1 (86-101)	88.6 (80-98)	87.3 (79-96)
SWEDEN	585.1 (525-659)**	494.7 (449-541)**	550.7 (508-591)**	563 (536-592)	602.8 (579-628)	668.5 (636-703)	691.9 (655-733)**	713.2 (676-754)**	707.1 (665-749)**	696.4 (652-742)**
Norra	506.2 (454-569)**	436.8 (398-477)**	486 (447-524)**	490.6 (467-514)	517.7 (497-541)	566.9 (538-597)	585 (550-622)**	604.9 (571-641)**	590.7 (552-630)**	566.3 (527-609)**
Jämtland	170.4 (146-195)	151.9 (134-170)	174.2 (158-190)	178.4 (164-193)	196.6 (184-211)	219.2 (203-236)	223.8 (209-240)	230.2 (217-244)	212.5 (197-228)	208.5 (193-224)
Norrbotten	180.5 (152-213)*	154.5 (130-181)*	166 (144-189)*	168.7 (158-181)	173.5 (163-185)	174.3 (160-192)	180.7 (158-206)*	185 (161-212)*	187.2 (160-216)*	183.8 (157-211)*
Västerbotten	131.7 (117-149)	110.6 (100-122)	124.7 (112-138)	117 (107-130)	112.3 (101-125)	132.2 (120-145)	133.9 (124-145)	138.5 (127-150)	125.3 (111-140)	121.8 (108-137)
Västernorrland	23.7 (15-32)	19.8 (13-27)	21.1 (14-29)	26.5 (19-34)	35.3 (29-43)	41.2 (34-49)	46.5 (39-54)	51.2 (44-59)	65.7 (58-74)	52.2 (44-61)
Mellersta	78.1 (61-98)	57.6 (46-70)	64.3 (53-76)	72.1 (61-83)	84.8 (76-95)	101.3 (90-113)	106.5 (94-118)	107.9 (96-119)	116 (105-128)	129.5 (117-143)
Dalarna	33.2 (24-44)	27.8 (21-35)	31.2 (25-39)	36.3 (30-44)	46.6 (41-53)	49.1 (42-57)	50 (42-58)	53.2 (46-61)	56.4 (49-63)	61.7 (55-69)
Gävleborg	17.4 (9-26)	13.8 (8-21)	16 (10-23)	18.4 (12-25)	22.1 (16-28)	35.5 (30-41)	35.4 (30-42)	34.1 (28-40)	33.1 (27-40)	39.8 (34-46)
Örebro	5 (1-10)	2.5 (0-6)	2.1 (0-5)	1.7 (0-4)	2 (0-5)	1.4 (0-4)	2.3 (0-5)	2.4 (0-6)	2.7 (0-6)	4.4 (1-9)
Stockholm	0.2 (0-1)	0.1 (0-1)	0.1 (0-1)	0.1 (0-1)	0.1 (0-1)	0.1 (0-1)	0.1 (0-1)	0.1 (0-1)	0.1 (0-1)	0.1 (0-1)
Uppsala	4.3 (1-9)	2.4 (0-6)	2.1 (0-5)	1.7 (0-5)	1.4 (0-4)	1.6 (0-5)	1.9 (0-5)	1.7 (0-5)	1.9 (0-5)	3.2 (0-7)
Värmland	13.7 (8-21)	8.5 (4-13)	10.8 (7-15)	12.1 (8-16)	11.3 (8-15)	12 (9-16)	14.9 (10-20)	14.6 (10-20)	20.1 (16-25)	16.9 (11-23)
Västmanland	2.4 (0-6)	1.3 (0-4)	1 (0-3)	0.9 (0-3)	0.7 (0-3)	0.8 (0-3)	1 (0-3)	0.9 (0-3)	1 (0-3)	1.7 (0-5)
VästraGötaland	2 (0-5)	1.1 (0-4)	1 (0-3)	0.9 (0-3)	0.7 (0-3)	0.8 (0-3)	0.9 (0-3)	0.9 (0-3)	0.9 (0-3)	1.6 (0-4)
Södra	0.7 (0-3)	0.4 (0-2)	0.3 (0-2)	0.3 (0-2)	0.3 (0-2)	0.3 (0-2)	0.4 (0-2)	0.4 (0-2)	0.4 (0-2)	0.6 (0-2)
Östergötland	0.3 (0-2)	0.2 (0-1)	0.2 (0-1)	0.2 (0-1)	0.2 (0-1)	0.2 (0-1)	0.2 (0-1)	0.2 (0-1)	0.2 (0-1)	0.3 (0-2)
Södermanland	0.4 (0-2)	0.2 (0-1)	0.2 (0-1)	0.2 (0-1)	0.1 (0-1)	0.2 (0-1)	0.2 (0-1)	0.2 (0-1)	0.2 (0-2)	0.3 (0-2)

**Table A.5:** Annual population growth rate estimates for the wolverine population in Scandinavia ("Total") and separately for Norway and Sweden. Estimates were derived using the posterior distributions of annual abundance estimates (Table A.4). Credible intervals (95%) are shown in parentheses.

	2014-2015	2015-2016	2016-2017	2017-2018	2018-2019	2019-2020	2020-2021	2021-2022	2022-2023
Norway	0.80 (0.73-0.89)	1.07 (0.98-1.16)	0.94 (0.88-1.01)	1.00 (0.95-1.07)	1.15 (1.08-1.22)	0.99 (0.93-1.05)	0.92 (0.86-0.98)	1.03 (0.97-1.10)	0.99 (0.93-1.05)
Sweden	0.85 (0.76-0.96)	1.11 (1.01-1.23)	1.02 (0.94-1.12)	1.07 (1.01-1.14)	1.11 (1.04-1.17)	1.04 (0.96-1.11)	1.03 (0.97-1.10)	0.99 (0.93-1.06)	0.99 (0.92-1.06)
Total	0.83 (0.75-0.91)	1.09 (1.01-1.18)	0.99 (0.93-1.06)	1.04 (1.00-1.09)	1.13 (1.07-1.18)	1.02 (0.96-1.07)	0.99 (0.94-1.04)	1.00 (0.95-1.06)	0.99 (0.93-1.04)

**Table A.6:** Estimates of the demographic parameters obtained from the sex-specific wolverine open-population spatial capture-recapture (OPSCR) models. Parameters represent transition rates from Dec 1 to Nov 30 in the following year. Median estimates and 95% credible intervals (in parentheses) for per capita recruitment rate ( $\rho$ ), survival ( $\phi$ ), mortality due to legal culling ( $h$ ), and mortality due to other causes ( $w$ ) are presented for males (M) and females (F). Note that mortality due to legal culling was not estimated directly in the model, but derived from the recorded number of dead recoveries.

	2014-2015		2015-2016		2016-2017		2017-2018		2018-2019	
	M	F	M	F	M	F	M	F	M	F
$\rho$	0.24 (0.15-0.34)	0.13 (0.04-0.24)	0.42 (0.32-0.52)	0.33 (0.22-0.44)	0.37 (0.29-0.45)	0.18 (0.11-0.26)	0.40 (0.34-0.46)	0.26 (0.20-0.32)	0.41 (0.35-0.48)	0.30 (0.24-0.36)
$\phi$	0.56 (0.49-0.64)	0.70 (0.63-0.77)	0.65 (0.58-0.72)	0.78 (0.72-0.84)	0.67 (0.61-0.73)	0.77 (0.71-0.82)	0.66 (0.60-0.71)	0.77 (0.72-0.81)	0.70 (0.64-0.75)	0.83 (0.78-0.88)
$h$	0.07 (0.06-0.08)	0.06 (0.05-0.07)	0.16 (0.15-0.18)	0.10 (0.09-0.11)	0.12 (0.11-0.13)	0.06 (0.06-0.07)	0.13 (0.12-0.13)	0.07 (0.06-0.07)	0.08 (0.08-0.09)	0.04 (0.04-0.04)
$w$	0.37 (0.31-0.42)	0.23 (0.17-0.30)	0.19 (0.14-0.24)	0.12 (0.07-0.18)	0.21 (0.17-0.26)	0.17 (0.12-0.22)	0.22 (0.19-0.25)	0.17 (0.13-0.20)	0.22 (0.19-0.25)	0.13 (0.09-0.17)
	2019-2020		2020-2021		2021-2022		2022-2023			
	M	F	M	F	M	F	M	F		
$\rho$	0.37 (0.31-0.43)	0.25 (0.19-0.32)	0.35 (0.29-0.41)	0.23 (0.17-0.29)	0.37 (0.32-0.44)	0.20 (0.15-0.26)	0.44 (0.38-0.52)	0.27 (0.22-0.33)		
$\phi$	0.62 (0.56-0.67)	0.77 (0.72-0.82)	0.61 (0.56-0.66)	0.77 (0.72-0.83)	0.63 (0.58-0.69)	0.79 (0.73-0.85)	0.65 (0.59-0.71)	0.64 (0.58-0.71)		
$h$	0.08 (0.08-0.08)	0.07 (0.06-0.07)	0.16 (0.15-0.17)	0.06 (0.06-0.07)	0.11 (0.10-0.11)	0.05 (0.05-0.06)	0.08 (0.08-0.09)	0.07 (0.07-0.08)		
$w$	0.30 (0.27-0.34)	0.16 (0.12-0.20)	0.23 (0.20-0.27)	0.16 (0.12-0.21)	0.26 (0.22-0.29)	0.16 (0.10-0.21)	0.27 (0.23-0.31)	0.28 (0.23-0.34)		

**Table A.7:** Estimates of the density and movement process parameters obtained from the sex-specific wolverine open-population spatial capture-recapture (OPSCR) models.  $\beta_{dens}$  represents the effect of the number of known wolverine dens on activity center locations (Bischof et al., 2020b). The scale parameter  $\sigma$  of the detection function is expressed in kilometers and estimated separately for each year.  $\lambda$  (in km) represents the mean of the exponential movement parameter, describing individual movement distances between years. Credible intervals (95%) are shown in parentheses. Parameters that were not estimated separately each year are marked with \*.

	2014		2015		2016		2017		2018	
	M	F	M	F	M	F	M	F	M	F
$\beta_{dens}^*$	0.44 (0.41-0.47)	0.52 (0.49-0.55)	0.44 (0.41-0.47)	0.52 (0.49-0.55)	0.44 (0.41-0.47)	0.52 (0.49-0.55)	0.44 (0.41-0.47)	0.52 (0.49-0.55)	0.44 (0.41-0.47)	0.52 (0.49-0.55)
$\sigma$	8.36 (7.93-8.81)	5.94 (5.60-6.33)	8.55 (8.12-9.02)	5.69 (5.37-6.04)	8.29 (7.91-8.69)	6.17 (5.83-6.53)	8.41 (8.09-8.74)	6.58 (6.30-6.86)	8.02 (7.75-8.29)	6.24 (5.99-6.51)
$\lambda^*$	14.66 (14.05-15.21)	7.85 (7.56-8.15)	14.66 (14.05-15.21)	7.85 (7.56-8.15)	14.66 (14.05-15.21)	7.85 (7.56-8.15)	14.66 (14.05-15.21)	7.85 (7.56-8.15)	14.66 (14.05-15.21)	7.85 (7.56-8.15)
	2019		2020		2021		2022		2023	
	M	F	M	F	M	F	M	F	M	F
$\beta_{dens}^*$	0.44 (0.41-0.47)	0.52 (0.49-0.55)	0.44 (0.41-0.47)	0.52 (0.49-0.55)	0.44 (0.41-0.47)	0.52 (0.49-0.55)	0.44 (0.41-0.47)	0.52 (0.49-0.55)	0.44 (0.41-0.47)	0.52 (0.49-0.55)
$\sigma$	7.78 (7.49-8.07)	5.64 (5.39-5.90)	8.00 (7.69-8.33)	6.26 (5.98-6.57)	8.06 (7.77-8.37)	6.35 (6.07-6.66)	8.07 (7.78-8.37)	5.76 (5.50-6.04)	8.27 (7.99-8.56)	6.62 (6.38-6.89)
$\lambda^*$	14.66 (14.05-15.21)	7.85 (7.56-8.15)	14.66 (14.05-15.21)	7.85 (7.56-8.15)	14.66 (14.05-15.21)	7.85 (7.56-8.15)	14.66 (14.05-15.21)	7.85 (7.56-8.15)	14.66 (14.05-15.21)	7.85 (7.56-8.15)

**Table A.8:** Estimates of the detection process parameters for the structured sampling.  $\beta_{1Structured}$  corresponds to the effect of previous detection of an individual,  $\beta_{2Structured}$  to the effect of search-effort (track length), and  $\beta_{3Structured}$  to the effect of average snow cover during the monitoring period on baseline detection probability ( $p_{0Structured}$ ). Coefficients are associated with scaled covariates. Credible intervals (95%) are shown in parentheses.

	2014		2015		2016		2017		2018	
	M	F	M	F	M	F	M	F	M	F
$\beta_{1Structured}$	1.02 (0.78-1.27)	0.66 (0.41-0.92)	0.44 (0.18-0.70)	0.05 (-0.21-0.33)	0.54 (0.32-0.76)	0.28 (0.03-0.53)	0.49 (0.31-0.67)	0.04 (-0.15-0.22)	0.54 (0.38-0.71)	0.14 (-0.05-0.33)
$\beta_{2Structured}$	0.49 (0.42-0.57)	0.46 (0.38-0.54)	0.50 (0.40-0.61)	0.48 (0.39-0.58)	0.48 (0.42-0.56)	0.54 (0.45-0.63)	0.50 (0.43-0.57)	0.46 (0.40-0.53)	0.46 (0.40-0.53)	0.49 (0.41-0.56)
$\beta_{3Structured}$	0.47 (0.17-0.78)	0.52 (0.21-0.85)	0.02 (-0.19-0.23)	0.19 (-0.03-0.40)	0.26 (0.03-0.48)	0.12 (-0.11-0.36)	0.31 (0.14-0.49)	0.23 (0.06-0.40)	0.13 (0.01-0.25)	0.02 (-0.12-0.16)
	2019		2020		2021		2022		2023	
	M	F	M	F	M	F	M	F	M	F
$\beta_{1Structured}$	0.59 (0.41-0.77)	0.17 (-0.02-0.36)	0.19 (0.02-0.37)	-0.06 (-0.26-0.13)	0.46 (0.28-0.64)	-0.14 (-0.34-0.06)	0.40 (0.23-0.58)	0.06 (-0.13-0.25)	0.55 (0.38-0.72)	0.18 (0.01-0.36)
$\beta_{2Structured}$	0.53 (0.46-0.60)	0.52 (0.45-0.60)	0.46 (0.40-0.53)	0.52 (0.44-0.59)	0.59 (0.51-0.68)	0.60 (0.53-0.68)	0.51 (0.44-0.60)	0.51 (0.44-0.59)	0.46 (0.40-0.52)	0.51 (0.44-0.58)
$\beta_{3Structured}$	-0.12 (-0.27-0.03)	-0.04 (-0.20-0.13)	0.32 (0.14-0.50)	0.41 (0.18-0.65)	0.15 (0.02-0.29)	0.24 (0.08-0.40)	0.08 (-0.06-0.23)	0.04 (-0.12-0.20)	0.40 (0.21-0.59)	0.35 (0.15-0.56)



**Table A.9:** Estimates of the detection process parameters for the unstructured sampling.  $\beta_{1Unstructured}$  corresponds to the effect of previous detection,  $\beta_{2Unstructured}$  to the effect of distance to the nearest road,  $\beta_{3Unstructured}$  to the effect of average snow cover during the monitoring period, and  $\beta_{4Unstructured}$  to the effect of spatio-temporal heterogeneity in unstructured sampling derived using the observation data in Skandobs and Rovbase on baseline detection probability ( $p_{0Unstructured}$ ). Coefficients are associated with scaled covariates. Credible intervals (95%) are shown in parentheses.

	2014		2015		2016		2017		2018	
	M	F	M	F	M	F	M	F	M	F
$\beta_{1Unstructured}$	0.54 ( 0.20-0.87)	0.38 ( 0.02-0.73)	0.08 (-0.23-0.40)	0.26 (-0.10-0.61)	0.44 ( 0.14-0.74)	0.35 ( 0.00-0.71)	0.18 (-0.07-0.43)	-0.24 (-0.52-0.03)	0.88 ( 0.65-1.13)	0.17 (-0.08-0.42)
$\beta_{2Unstructured}$	0.51 ( 0.18-0.87)	0.59 ( 0.25-0.96)	0.29 ( 0.05-0.54)	0.51 ( 0.26-0.78)	0.03 (-0.19-0.26)	0.32 ( 0.06-0.58)	0.48 ( 0.26-0.71)	0.34 ( 0.11-0.56)	0.21 ( 0.05-0.38)	0.17 ( 0.00-0.35)
$\beta_{3Unstructured}$	0.12 (-0.07- 0.31)	0.24 ( 0.05-0.41)	-0.02 (-0.24- 0.19)	0.07 (-0.14-0.26)	0.02 (-0.19- 0.22)	-0.17 (-0.42-0.05)	0.03 (-0.07- 0.14)	0.11 ( 0.01-0.21)	-0.04 (-0.14- 0.06)	-0.02 (-0.13-0.08)
$\beta_{4Unstructured}$	0.70 ( 0.36-1.04)	0.49 (0.16-0.82)	0.44 ( 0.12-0.75)	0.72 (0.38-1.07)	0.69 ( 0.38-1.01)	0.35 (0.02-0.69)	0.51 ( 0.26-0.76)	0.50 (0.24-0.76)	0.63 ( 0.39-0.88)	0.86 (0.59-1.14)
	2019		2020		2021		2022		2023	
	M	F	M	F	M	F	M	F	M	F
$\beta_{1Unstructured}$	0.43 ( 0.13-0.74)	0.04 (-0.25-0.34)	0.38 ( 0.12-0.65)	0.11 (-0.20-0.42)	0.69 ( 0.43-0.95)	0.55 ( 0.23-0.86)	0.79 ( 0.51-1.09)	0.19 (-0.14-0.53)	0.74 ( 0.48-1.00)	0.32 ( 0.02-0.63)
$\beta_{2Unstructured}$	0.05 (-0.19-0.29)	0.18 (-0.06-0.42)	0.28 ( 0.04-0.52)	0.47 ( 0.15-0.83)	0.14 (-0.05-0.33)	-0.02 (-0.24-0.20)	0.19 (-0.02-0.41)	0.05 (-0.19-0.30)	0.45 ( 0.20-0.72)	0.10 (-0.17-0.39)
$\beta_{3Unstructured}$	0.00 (-0.17- 0.15)	-0.06 (-0.22-0.09)	-0.16 (-0.38- 0.04)	-0.19 (-0.43-0.03)	-0.08 (-0.29- 0.11)	-0.04 (-0.25-0.15)	-0.29 (-0.55-0.07)	-0.14 (-0.39-0.09)	-0.02 (-0.22- 0.16)	0.06 (-0.13-0.24)
$\beta_{4Unstructured}$	0.74 ( 0.41-1.07)	1.02 (0.68-1.39)	0.25 (-0.03-0.52)	0.33 (0.02-0.66)	0.56 ( 0.28-0.86)	0.71 (0.37-1.07)	0.37 ( 0.06-0.67)	0.59 (0.22-0.96)	0.57 ( 0.31-0.84)	0.47 (0.15-0.81)

**Table A.10:** Average proportion of individuals detected via non-invasive genetic sampling (NGS) in Sweden and Norway for males (M) and females (F). Values were calculated as the number of individuals detected with NGS (Table A.2) divided by the total and sex-specific abundance estimates obtained from the open-population spatial capture-recapture (OPSCR) models (Table A.4). Credible intervals (95%) are shown in parentheses. Note that in some years in Norway, male wolverines detected exceeded the estimated number of wolverines. This is possible when wolverine detection probability was very high and wolverines with activity centers in Sweden were detected on the Norwegian side of the border.

	2014		2015		2016		2017		2018	
	F	M	F	M	F	M	F	M	F	M
Norway	0.66 (0.59-0.74)	0.84 (0.75-0.94)	0.66 (0.60-0.73)	0.91 (0.83-0.98)	0.71 (0.65-0.76)	0.95 (0.88-1.02)	0.77 (0.73-0.82)	1.05 (0.99-1.12)	0.73 (0.68-0.77)	0.98 (0.92-1.03)
Sweden	0.24 (0.20-0.28)	0.31 (0.26-0.37)	0.35 (0.31-0.39)	0.46 (0.40-0.52)	0.31 (0.28-0.35)	0.51 (0.46-0.56)	0.63 (0.58-0.67)	0.78 (0.74-0.83)	0.65 (0.61-0.69)	0.85 (0.81-0.89)
Total	0.42 (0.37-0.47)	0.53 (0.47-0.60)	0.48 (0.43-0.52)	0.62 (0.56-0.67)	0.48 (0.44-0.51)	0.67 (0.62-0.71)	0.66 (0.62-0.69)	0.82 (0.78-0.86)	0.66 (0.63-0.69)	0.84 (0.81-0.87)
	2019		2020		2021		2022		2023	
	F	M	F	M	F	M	F	M	F	M
Norway	0.73 (0.69-0.77)	0.97 (0.91-1.04)	0.76 (0.71-0.81)	0.98 (0.92-1.04)	0.78 (0.73-0.83)	0.98 (0.92-1.05)	0.78 (0.72-0.83)	0.99 (0.93-1.05)	0.91 (0.85-0.97)	1.03 (0.96-1.09)
Sweden	0.56 (0.52-0.60)	0.74 (0.69-0.79)	0.40 (0.37-0.43)	0.60 (0.55-0.65)	0.46 (0.43-0.49)	0.64 (0.58-0.69)	0.44 (0.41-0.48)	0.67 (0.62-0.72)	0.49 (0.44-0.54)	0.65 (0.60-0.70)
Total	0.61 (0.58-0.65)	0.80 (0.76-0.84)	0.53 (0.50-0.56)	0.73 (0.69-0.77)	0.56 (0.53-0.59)	0.74 (0.70-0.78)	0.56 (0.53-0.60)	0.75 (0.71-0.80)	0.63 (0.58-0.68)	0.75 (0.71-0.80)